UNIVERSITY OF NAIROBI

SYNTHESIS AND CHARACTERIZATION OF IRON NANOPARTICLES USING BANANA PEELS EXTRACTS AND THEIR APPLICATION IN APTASENSOR

By

ONDIEK JOHN K. OKOTH

A thesis submitted in partial fulfilment of the requirements for the award of the degree of Masters of Science (Analytical chemistry) of the University of Nairobi

November, 2016

DECLARATION

I declare that **'synthesis and characterization of iron nanoparticles using banana peels extracts and their application in aptasensor'** is my original work and has not been submitted for any degree or examination in this university or any other institution of learning and that all the resources I have used or quoted have been indicated and acknowledged by means of complete references.

Signature…… Date.....……

ONDIEK JOHN K.OKOTH - I56/79300/2012
DEPARTMENT OF CHEMISTRY
UNIVERSITY OF NAIROBI

This thesis has been submitted for examination with our approval as the University supervisors.

Signature…… Date.....……

PROF. G. N. KAMAU
DEPARTMENT OF CHEMISTRY
UNIVERSITY OF NAIROBI

Signature…… Date.....……

DR. IMMACULATE MICHIRA
DEPARTMENT OF CHEMISTRY
UNIVERSITY OF NAIROBI

Signature…… Date.....……

DR. PETERSON M. GUTO
DEPARTMENT OF CHEMISTRY
UNIVERSITY OF NAIROBI

DEDICATION

I dedicate this work to my wife Jedida, Daughter Toppy, Son Pepe and to everyone who contributed to its success.

ACKNOWLEDGEMENTS

I thank God Almighty for giving me strength and resilience to complete this work. I sincerely extend my heartfelt gratitude to my supervisors and advisors: Prof. G. N. Kamau, University of Nairobi; Prof. Emmanuel I. Iwuoha, University of Western Cape (SA); Dr. P. Guto, University of Nairobi; Dr. Immaculate Michira, University of Nairobi. Thank you very much for all your encouragements, talks, academic and technical support during this research work.

I also wish to thank the entire staff of chemistry department, University of Nairobi for their tireless efforts and working closely with me during my research. I acknowledge SensorLab research group, University of Western Cape (SA), especially Dr. Tesfaye Waryo and Dr. Masikini Milua for their contribution and assistance they made in this work. Thank you very much for creating conducive research environment. To the Nanotechnologists Moses Oyagi, Joshua Sila and Phillis Emelder, thank you so much. Family members, relatives and friends, I thank you for your support throughout my studies.

Special thanks to Southern and Eastern Africa Network of Analytical Chemists (SEANAC), SensorLab, University of Western Cape and University of Nairobi for the financial assistance during my research work. May almighty God bless you abundantly.

ABSTRACT

Bio-inspired Iron nanoparticles were successfully synthesized by reduction of ferric chloride solution using aqueous solution of banana peel extract (BPE). The method was non-lethal, simple, eco-accommodating and relatively inexpensive. The resulting iron nanoparticles were characterized by physical colour changes, Fourier-transform infrared (FTIR) spectroscopy, UV-Vis spectroscopy, transmission electron microscopy (TEM), Energy Dispersive X-Ray (EDX), Scanning Electron Microscopy (SEM) and X-Ray Diffraction (XRD). The reaction mixture of aqueous ferric chloride and BPE displayed observable colours confirming the synthesis of Iron nanoparticles. UV–Vis spectra showing an absorption band at 276nm characteristic of the iron nanoparticles in deed revealed the presence of nanoparticles.

Images of the biosynthesized Iron nanoparticles at different magnifications from SEM showed that the particles were round in shape with smooth surfaces. The TEM images revealed the nanoparticles were granular in nature with sizes in the range of 20-50 nm. EDX had strong iron signals at 182, 215, 424 and 458 energies, thus confirming the synthesis of Iron nanoparticles.

X-ray diffraction investigations of the BPE synthesized Iron nanoparticles revealed that the nanoparticles were amorphous in nature with crystal planes at (110), (200) and (112) characteristic for iron nanoparticles. Fourier transform infrared (FTIR) spectroscopy showed the contribution of phenols, nitriles and carboxylic groups in the synthesis procedure.

An aptasensor was developed using cyclic voltammetry as a transducer for the detection of microcystin-LR (MC-LR) by immobilizing MC-LR targeting aptamers onto electro-deposited polyaniline (PANI) doped with synthesised iron nanoparticles (FeNPs). Aptamer microcystin binding event was monitored and recorded by cyclic voltammetry. The linear range (LR) and the limit of detection (LOD) of the aptasensor were from 0.2 – 1 μgL^{-1} and 0.06 $\mu molL^{-1}$ respectively.

The World Health Organization (WHO) has set a concentration limit of 1µmol L^{-1} for MC-LR in drinking water while the method developed in this work could easily detect MC-LR with good sensitivity and linearity down to the nanomolar range.

TABLE OF CONTENTS

LIST OF FIGURES

LIST OF TABLES

LIST OF SCHEMES

LIST OF ABBREVIATIONS

BPE	Banana Peels Extracts
CV	Cyclic Voltammetry
DLS	Dynamic Light Scattering
ELISA	Enzyme-Linked Immunosorbent Assays
FTIR	Fourier Transform Infrared
HPLC	High Performance Liquid Chromatography
JCPDS	Joint Committee Centre Diffraction Data
LC	Liquid Chromatography
LD	Lethal Dose
LSV	Linear Sweep Voltammeter
MC	Microcystin
MC-LR	Microcystin-LR
Mm	Milli moles
Mv	Milli volts
Nm	Nanometre
NPs	Nanoparticles
PANI	Polyaniline
PANSA	Poly (8-anilino-1-naphthalene sulphonic acid)
PCZ	Polycarbozole
PEG	Polyethylene glycol
PL	Photolumiscence
PLD	Pulsed Laser Deposition

PND	Polyindole
PPIA	Protein Phosphate Inhibition Assays
PPY	Polypyrrole
Pt	Platinum
PVP	Polyvinylpyrrollidone
SPR	Surface Plasmon Resonance
SAED	Selected Area Electron Diffraction
SEM	Scanning Electron Microscope
SWV	Square Wave Voltammeter
TEM	Transmission Electron Microscope
µl	Micro litre
UV-Vis	Ultraviolet visible spectroscopy
WHO	World Health Organisation
XRD	X-ray diffraction

CHAPTER ONE

INTRODUCTION

1.1 Nanoparticles.

Nano means very small and thus Nanoparticles are small particles of substances that behave in general as far as its properties. Nanoparticles are the building blocks of nanotechnology. Nanotechnology is the study of manipulating matter on a nuclear and sub atomic scale levels. Generally, nanotechnology manages structures measured between 1-100 nanometres. Nanotechnology is a quickly developing area of exploration on the planet today. The research explosion in this field is because these particles have exceedingly better characteristics than their macroscale counterparts. For example, they have found great use in the worlds of technology, medicine, computers, biosensors and environmental remediation.

1.2 Iron nanoparticles

Iron nanoparticles innovation represents perhaps one of the first generation nanoscale natural advances. In the course of the most recent couple of years, different engineered strategies have been created to deliver iron nanoparticles, adjust the nanoparticles surface properties and improve the productivity for field conveyance and responses. While several types of iron nanoparticles are available in the market, information on the nanoparticles synthesis and properties is still limited in journals. Chemical (Chou *et al*., 2005) and physical methods (Lin and Yang, 2006) have been applied to synthesize metallic nanoparticles of specific sizes and morphologies. These methods employ harmful chemicals such as sodium borohydride, sodium citrate dihydrate which are possibly hazardous and very costly to the natural settings and organic functions (Dubey *et al*., 2010).

Bio inspired synthesis of these particles proves to be cost effective environmental alternative to chemical and physical methods in preparing of nanoparticles. Banana peels contains diverse high levels of phenolic compounds that can act as both reducing and capping agents hence afford a green synthetic approach. (Dubey *et al*., 2010).

1.3 Microcystin - LR

Cyanobacteria, sometimes known as blue-green algae, consist of a family of one celled algae that grow in lakes, slow-moving streams, ponds and other water reservoirs. They thrive in warm and nutritious waters producing a cluster of toxins known as microcystin. Microcystins are cyclic peptides having approximately eighty structural variants and commonly found in water bodies throughout the world. The most common of these variants is Microcystin-LR, Microcystin-YR, Microcystin-RR, and Microcystin-LW. Some of these microcystin are toxic and upon ingestion by fish, mammals and birds predominantly affect the liver, resulting into minor to extensive damage. Water-skiing, swimming or boating in Microcystins contaminated water can lead to the exposure to the toxins. These toxins may also be found in fish that are taken from such contaminated water. Reports by World Health Organisation (WHO) have indicated that livestock and pets have died after consuming Microcystins contaminated water. A large population of the world relies on surface waters as their main source of drinking water. Toxic cyanobacteria are increasing in most surface waters worldwide because of increased nutrient pollution resulting from eutrophication (Niazi *et al*., 2008).

1.4 Application of Iron nanoparticles

Nanomaterials have attracted immense attention as it can improve the sensitivity as well as the stability of the biosensors in view of their incredible electrical properties. These materials are biocompatible and because of their substantial surface area to volume proportion they are usually used in immobilization of aptamers so as to increase the surface density of the aptamers. Aptamers immobilised on nanoparticles have increased performance, stability as well as signal amplification. As an alternative to antibodies, aptamers bind targets with specificity and affinity that is comparable to monoclonal antibodies. In addition, they have longer shelf-life; can be engineered easily and are resistant to degradation and denaturation. The aptamer target binding have been sensed through surface Plasmon resonance (SPR) (Niazi *et al*., 2008) and fluorescence approach (Zhang *et al*., 2011; Zhao *et al*., 1999). Until now, few studies have reported on the use of electrochemistry in the transduction of the aptamer target binding events on electrode surface. This research work reports iron nanoparticles aptamer linked biosensor that can detect microcystin - LR by measuring the electrochemical response of the microcystin–aptamer complex.

1.5 Problem statement

Compound and physical techniques have been used in synthesis of iron nanoparticles (FeNPs) of particular sizes and configurations. These techniques utilise lethal chemicals such as stabilizing agents, non-biodegradable reducing agents or organic solvents which are hazardous to the earth and organic systems which are costly and time consuming. In the present work, bio synthesis of nanoparticles has been proposed as a financially savvy ecological contrasting option to compound and physical techniques.

Banana peels forms 18-33% (Best *et al.*, 1984) of the whole fruit and at present, they aren't being utilised for any other purposes if not dumped as solid waste at large expense to the environment or fed to animals to a limited extent. It is consequently critical and even crucial to discover applications for these peels as they can add to genuine ecological issues.

Surface waters are currently the main source of drinking water for a large population of the world but due to increased nutrient pollution resulting from eutrophication, most of these surface waters contain toxic Microcystins. These Microcystins upon ingestion by fish, mammals and birds affects the liver, resulting into death or extensive liver damage. Thus there is need to detect the Microcystins in water that is used for drinking.

Different methods have been employed in the sensing of microcystin including enzyme linked Immunosorbent assay (ELISA) and neuroreceptor assays (NRA). ELISA and NRA require antibodies and sensitive neuroreceptors that are expensive and require extensive sample preparation. Since microcystin poisons have adverse effect on human, a quick and relatively cheap detection tool needs to be established with suitable procedures to monitor the toxins in drinking water. Aptamers were chosen as good sensors as they have longer shelf life, are resistant to degradation and denaturation as well as can be engineered easily as compared to antibodies and neuroceptors. In addition, the aptamers decreases the time and cost for screening water samples for microcystin.

This work concentrated on the development of iron nanoparticles based aptamer for determination of microcystin-LR (MC-LR). The aptamer based nanobiosensor systems was prepared with aptamer deposited on glassy carbon electrode (GCE) electro catalytically activated with metalized polymeric nanocomposites system. The polymeric nanocomposites

system was synthesised with polyaniline (PANI) and metalized with iron nanoparticles (FeNPs). The sensor response profile was monitored using cyclic voltammetry (CV).

1.6 Objectives

1.6.1 Overall objective

The overall aim of this study was to synthesize iron nanoparticles through bio inspired synthetic approach, characterize them and investigate their application in aptasensor for Microcystin-LR detection.

1.6.2 Specific objectives

1. To synthesize iron nanoparticles using aqueous Banana peels extracts.
2. To characterize the iron nanoparticles using different analytical techniques.
3. Investigate the applicability of the synthesized iron nanoparticles in aptasensor.

1.7 Significance of the study

Nanotechnology innovation is the quickest developing divisions of technology with multiple consumer products. Its little size and extensive surface area per unit volume imparts characteristics that can be useful in aptasensor construction. Iron nanoparticles (FeNPs) application is a very promising, efficient and cost effective method for remediating this environmental health concern. There is a need therefore to develop environment friendly procedures for synthesizing FeNPs devoid of toxic by-products, high pressure, energy and temperature inputs. Banana peels extracts have shown prospects in FeNPs synthesis which is a ‘green chemistry’ synthetic approach.

Aptamers are relatively cheap, quick and sensitive method of monitoring microcystin in open surface water and thus can be employed to avoid deaths associated with microcystin poisoning.

CHAPTER TWO

LITERATURE REVIEW

2.1 Iron nanoparticles (FeNPs)

Iron is one of the low cost, non-toxic and the most common element. It forms structural backbone of modern infrastructure, coatings, textiles and specific alloys (Nuxoll *et al*., 2003). The technology of iron nanoparticle is one of the original nanoscale environmental technologies. Uses of metallic iron in environmental applications have been accepted by many users as well as regulatory agencies. The use of the metal has been widely reported in the form of permeable reactive barriers and packed bed reaction. At the nanoscale, Iron has a great deal to offer because of their enormous surface area of reactivity, high electrical, optical, magnetic and catalytic properties. These exclusive properties have been exploited for various uses as well as applications. In the recent works, Iron nanoparticles have been employed as potent magnets as well as catalyst. Research on the application of the nanoparticles across the broad array of environmental remediation have recently gained enormous interest among researchers, with one of the noticeable applications being in the evacuation of inorganic and natural contaminations from fluid arrangements (Arnold and Roberts, 2000). Iron nanoparticles have been utilised as a Fenton like catalyst in the degradation of organic solutes (Elliott and Zhang, 2006). A commercial technology has been the use of iron nanoparticles for the reduction of chlorinated organics in water (Senzaki and Kumagai 1988). Generally, iron nanoparticles have been used for contaminants like halogenated aliphatic, halogenated aromatics, brominated or carbarylated herbicides and pesticides, nitro aromatics, lead, mercury, arsenic and hexavalent chromium (Kumar, 2006; Lo *et al*. 2009).

Super paramagnetic iron oxide nanoparticles (SPIONs) synthesised with proper surface architecture are conjugated with targeting ligands/proteins and employed in drug delivery applications, magnetic resonance imaging (MRI) and in electrical components like the core of transformers and inductors (Gupta and Wells, 2004). The magnetic properties of Fe has made it one of the most popular choices in magnetic data storage and in electromagnets that require low energy loss as well as high susceptibility.

These versatile applications of the iron nanoparticles require an economic and well simplified synthesis technique of production with a high yield. Over the past few years, several synthetic methods have been established to produce iron nanoparticles, modify the surface properties of the nanoparticle and enhance the efficiency of the nanoparticles employed in the field of drug delivery and reactions. The twelve standards of green science have turned into an aide for scientific experts as well as chemical technologists in coming up with less hazardous chemical synthesis.

2.2 Methods of FeNPs synthesis

Two general methodologies of nanoparticle production are top-down and bottom-up methods. In top-down, large size materials generate nanoparticles through mechanical and synthetic strides including processing, vacuum sputtering and machining (Lin *et al*., 2006). Like when iron nanoparticles are formed by decomposing iron pentacarbonyl ($Fe(CO)_5$) in natural solvents (Karlsson *et al*., 2005). The bottom-up methodology involves growing of nanomaterials atom-by-atom or molecule-by-molecule through chemical synthesis and self-assembling among others. Scheme 2.1 demonstrates the bottom up and top down approaches of synthesizing nanoparticles.

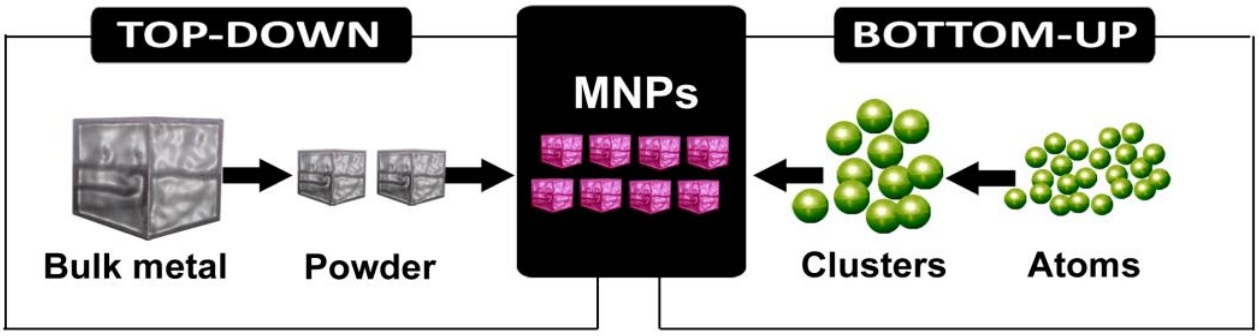

Scheme 2.1: The bottom up and top down approaches of synthesizing nanoparticles.

2.2.1 Synthesis using sodium borohydride

The production of iron nanoparticles by the "bottom-up" reduction of Iron three or Iron two salts with $NaBH_4$ is the popular method utilised by several researchers (Huber, 2005; Wang and Zhang, 1997). The iron ions are reduced according to the equation below:

$$4Fe^{3+} + 3BH^{-}_{4} + 9H_2O \rightarrow 4Fe^{0}\downarrow + 3H_2BO^{-}_{3} + 12H^{+} + 6H_2\uparrow \quad \ldots\ldots\ldots\ldots\ldots\ldots 1$$

In this case, $NaBH_4$ is employed as the reducing agent and iron nanoparticles with specific morphologies and sizes have been obtained. Essential health and security considerations must be made when borohydride reduction approach is used; the synthesis needs to be conducted in a fume chamber as Sodium Borohydride ($NaBH_4$) is highly toxic and corrosive. In addition, the hydrogen gas produced during the reaction as a by-product is highly flammable. Production of iron nanoparticles using this method is again expensive as blast resistant mixers must be utilised to reduce the likelihood of flashes due to flammable hydrogen.

2.2.2 Mechanical attrition

Mechanical attrition is a "top-down" process of producing nanoparticles of different sizes and shapes. The nanoparticles are synthesised in a mechanical device known as a "mill". Energy is imparted in this mill device so as to coarse grain a material thereby effecting a

reduction in particle size. The subsequent particulate matter can show nanostructural properties on at least two levels. First, the particles themselves that usually possess a distribution of sizes may be "nanoparticles" when their characteristic dimensions (diameter for spherical particles) are less than 100 nm (Aki *et al.*, 2013). Secondly, many of these materials milled in mechanical attrition devices are crystalline such that after milling their crystalline are often between 1 and 10 nm in diameter.

Mechanical attrition is however costly, energy intensive and waste producing. In addition, Fe nanoparticles synthesised using these methods has been found to be not capped and subject to corrosion and combines with oxygen if dry.

2.2.3 Synthesis using electrochemical method

Iron nanoparticles have also been prepared from the reaction of ferric chloride solution with Aluminium powder in a simplified electrochemical route (Hadjipanayis and Siegel, 2012). The electrochemical reaction involves a difference in oxidation potentials between Al and Fe. Addition of Al powder into aqueous $FeCl_3$ solution leads to formation of iron particles in the solution. For this case, the extent of the particles was controlled by changing the reaction conditions. Fe nanoparticles are prevented from oxidation by the hydrogen produced during the reaction. Scanning electron microscopy, X-ray analysis and energy dispersive have been used to characterise iron nanoparticles synthesised through electrochemical methods.

These methods present various limitations and problems; the bottom-up approaches have safety issues that are related to flammable hydrogen gas produced during the process and the toxicity of sodium borohydride as well as the formation of large agglomerates. Top-down methods on the other hand require specific equipment that are generally complex, expensive, energy consuming and often involve multiple steps. The disadvantage of the electrochemical

methods of synthesising iron nanoparticles is the formation of aggregates of the nanoparticles at the cathode's motor.

These disadvantages creates an incentive to employ green chemistry principles like the use of 'greener' solvents , reducing agents and capping agents (Hoag *et al*., 2009). It is apparent that nanoparticles have numerous applications and their production utilising simple techniques and cost effectiveness is of great significance.

2.2.4 Use of plant extracts

Bio synthesis of nanoparticles by plant extracts is currently under exploitation and is conceivably beneficial than elaborate process of maintaining cell cultures when using microorganisms. The use of *Azadirachtaindica* (Neem), *Medicago sativa* (Alfalfa), *Aloe vera* and microorganisms (Duran *et al*., 2005; Narayanan and Sakthivel. 2010; De souza, 2007) has already been reported for the creation of gold and silver nanoparticles.

2.2.5 Synthesis of Iron nanoparticles using plant extracts

FeNPs of various dimensions and morphologies have been manufactured using aqueous tea extracts. According to previous research (Shahwan *et al*., 2011), the polyphenol compounds and the water soluble constituents are mainly accountable for the reduction of metal ions and stabilization of the nanoparticles respectively. Reductase (Kumar *et al*., 2008) and

polysaccharides (Huang *et al.*, 2015) are reported to be the major factors involved in biosynthesis. Green tea-catechins (GTCs) are groups of Polyphenols compounds belonging to the flavonoid family. They include; (-)-epigallocatechin (EGC), (-)-epigallocatechin-3-gallate (EGCG), epicatechin (EC), (-)-epicatechin-3- gallate (ECG) and possesses various biological activities (figure 2.1). The synthesized iron nanoparticles using tea extracts were found to be nontoxic and more effective as a Fenton-like catalyst.

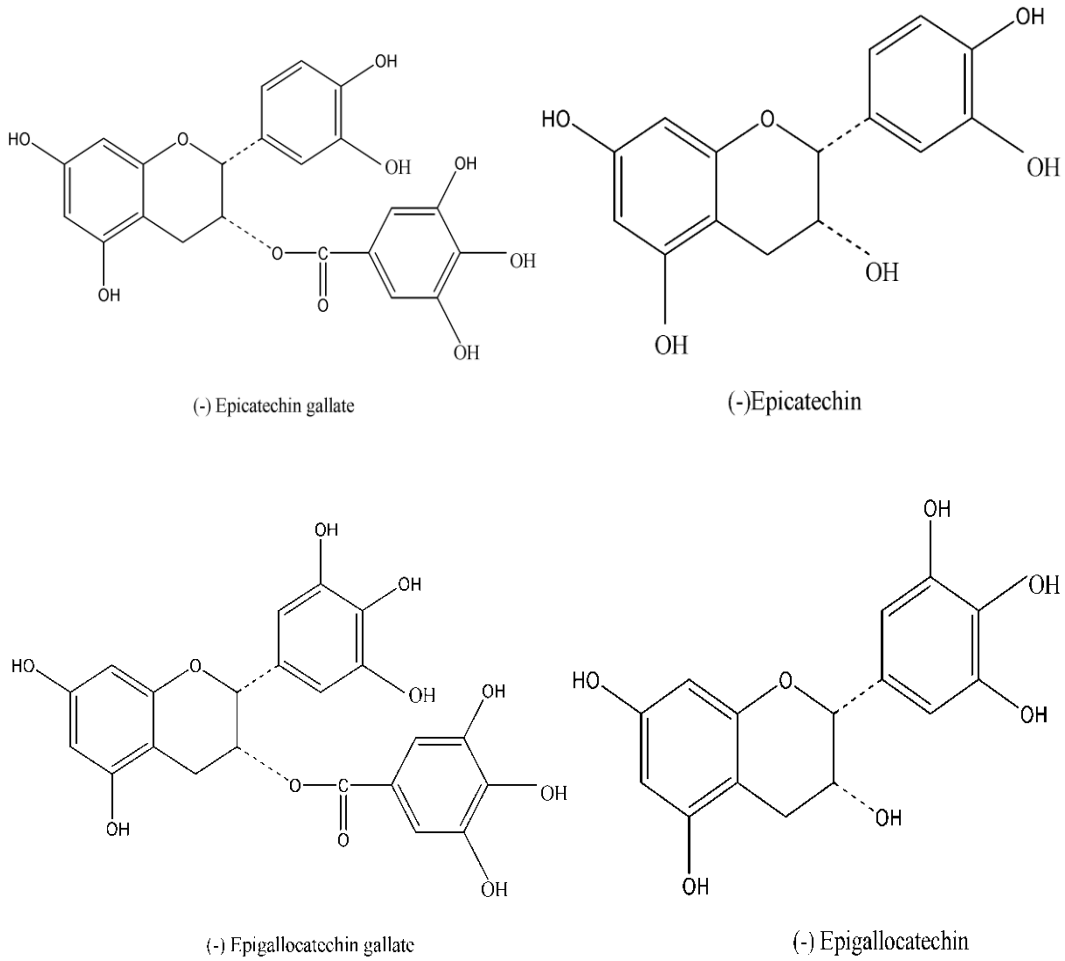

Figure 2.1: Structures (-)-Epicatechin-3-gallate (ECG) , (-)-Epicatechin (EC), (-)-Epigallocatechin-3-gallate (EGCG) and (-) Epigallocatechin (EGC).

Pattanayak and Nayak (2013) demonstrated that extract of Azadirachta indica (Neem plant) was capable of producing iron nanoparticles with good stability in solution and with good surface Plasmon resonance. Neem plant leaves extract was used to reduce ferric chloride and remarkable change in colour with change in pH of solution observed. The synthesis was rapid, environmentally friendly and of low cost as compared to chemical synthesis protocols.

A simple, low-cost and eco-friendly approach of preparing of Fe_3O_4 nanoparticles using *Tridax procumbens* leaf extract was reported by Senthil and Ramesh (2012). Reduction of ferric chloride solution was achieved using *Tridax procumbens* extract as the reducing agent. The obtained Fe_3O_4 nanoparticles were characterised using XRD, SEM and FTIR techniques and its antibacterial effect investigated against *Pseudomonas aeruginosa*.

In producing nanoparticles using whole or part of plant cuttings, concentrates is mixed with metal salt solution at ambient conditions. Nature of the plant extract, temperature at which the reaction is carried out, its concentration and that of the metal salt, pH, reaction time are known to affect the rate of production of nanoparticles in terms of their quantity and characteristics (Njagi *et al*., 2011). The pH of the Chamomile extracts and green tea extracts were measured using the Accumet Model 15 pH meter and the results recorded. From the pH values of the tea extract, it is clear that the pH values decreased slightly with the increase in the temperature of extraction. This implies therefore that at higher temperatures, more of the phenolic compounds are extracted. Also green tea gave the most acidic extracts at different temperatures compared to the other three tea extracts at the corresponding temperatures implying that using green tea in the biosynthesis of the nanoparticles would produce better results (Njagi, *et al*., 2011).

Utilization of plant concentrates is entirely respectable prompting really green science which gives progression over synthetic and physical strategy as it is inexpensive, environmentally practical, easily topped up for bulky synthesis and does not require usage of high pressure, energy and temperature (Dubey *et al.*,2010). Scheme 2.2 illustrates general mechanism for synthesis of nanoparticles using plant extracts.

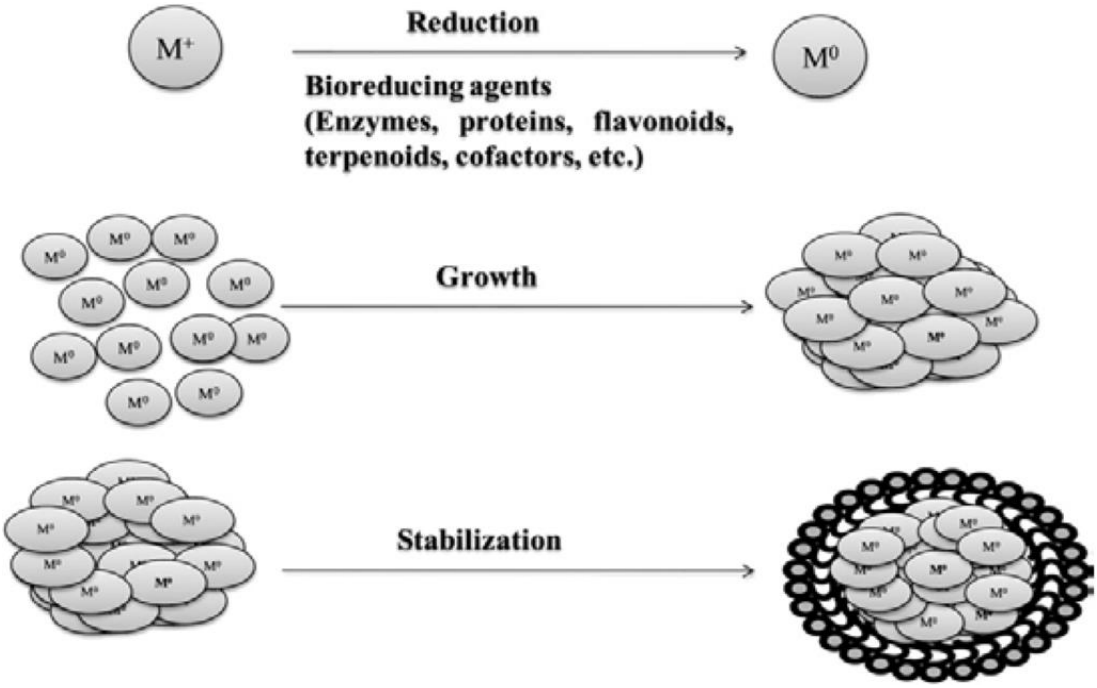

Scheme 2.2: General mechanism for synthesis of nanoparticles using plant extracts.

In this research work, aqueous Banana peels extracts was considered for the production of Iron nanoparticles.

2.3 Banana peels extract (BPE)

Banana (Musa *paradaisica*), belongs to the family *Musaceae* and is a standout amongst the most vital tropical fruits in the world market. It is become worldwide and devoured as ready organic product or utilized for culinary purposes. It is thus vital to find applications for the peels as they can add to real environmental complications (Best *et al.*, 1984). Banana peels contains large amounts of phenols which assists in creation of metallic nanoparticles (Bankar *et al.*, 2010).

Figure 2.2 shows Banana plant (A), banana fruits (B) and banana peels (C)

Figure 2.2: Banana plants (A), banana fruits (B) and banana peels (C).

Total phenolic and Gallocatechin have been reported (Someya, *et al.*, 2002) and are found to be more abundant in peels than in pulp making the Banana peels a better antioxidant. Evidence indicates that Banana peels extracts have very powerful free radical scavenging properties in vitro (Mokbel and Hashinaga, 2005).

The peels of banana are usually discarded though their therapeutic worth has been discovered (Best *et al*., 1984) and they have also been used as substrates for the production of fungal biomass (Mokbel and Hashinaga, 2005). In this work, we explain a fresh natural way for the biosynthesis of Fe nanoparticles using the banana peel extract (BPE).

2.3.1 Synthesis of nanoparticles using banana peels extract

Banana peel waste concentrate has been used in the synthesis of palladium nanoparticles in a novel biological route (Bankar *et al*., 2010). The researchers hypothesized that the banana peel extract (BPE) composed of polymers like lignin, pectin and hemicelluloses that could have aided the synthesis of palladium nanoparticles.

BPE has also been used as an effective green material for quick production of gold nanoparticles (Bankar *et al*., 2010). Banana peels extract mediated the structuring of the

nanoparticles into micro wire networks and the resulting gold nanoparticles had antifungal as well as antibacterial activities towards pathogenic fungi and bacteria cultures.

Bhattacharya and Mukherjee (2008) have also used banana peel extract for quick synthesise of various nanoparticles. They used different reaction conditions to produce silver nanoparticles that are used in areas of microelectronics, bio diagnostics, sensing, imaging and designing of newer drugs.

The use of banana peels extract has thus been shown to be non-toxic, simple, eco-friendly and low cost method of synthesising nanoparticles and could replace the cost intensive conventional methods of producing nanoparticles. In addition, the banana peels are abundantly obtainable 'green' agricultural waste materials that are usually discarded.

2.4 Microcystins

Microcystins are heptapeptides produced by various bloom-forming cyanobacteria commonly found in fresh-water bodies (Figure 2.3). They are cyclic in nature (Figure 2.4) with specific nomenclature depending on the varying amino acids that it is composed of (Messineo *et al.*, 2009).

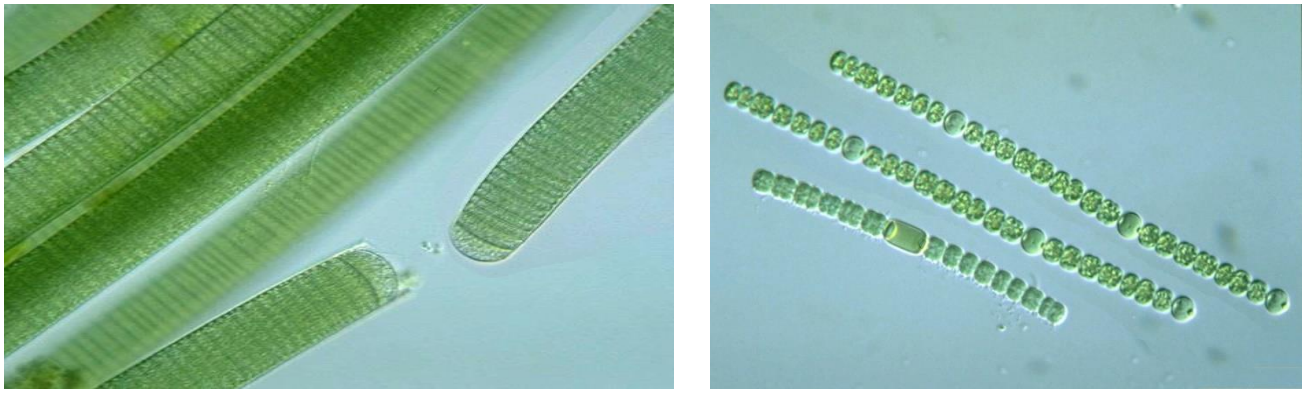

Figure 2.3: Photographs of cyanotoxins producing cyanobacteria.

Among the various microcystin, the microcystin-LR (MC-LR) is the frequently occurring and very poisonous microcystin (Figure 2.4). It is released in considerable amounts through the bacterial cell lysis. It is chemically stable, highly soluble in water and can survive in the surface water bodies for a long time. The Microcystins poisons can chemically decompose at high temperatures (40°C) or at either very high pH (>9) or low (<1) (Lahti *et al.,* 1997). The half-life at pH 1 and 40^{o}C is approximately three weeks while at ambient conditions the half-life is ten weeks. The toxins can stay for months or years when released into dark, cooler and natural water bodies. The toxins have been shown to persist even after boiling, implying that cooking does not destroy the toxins (Mountfort *et al*., 2005).

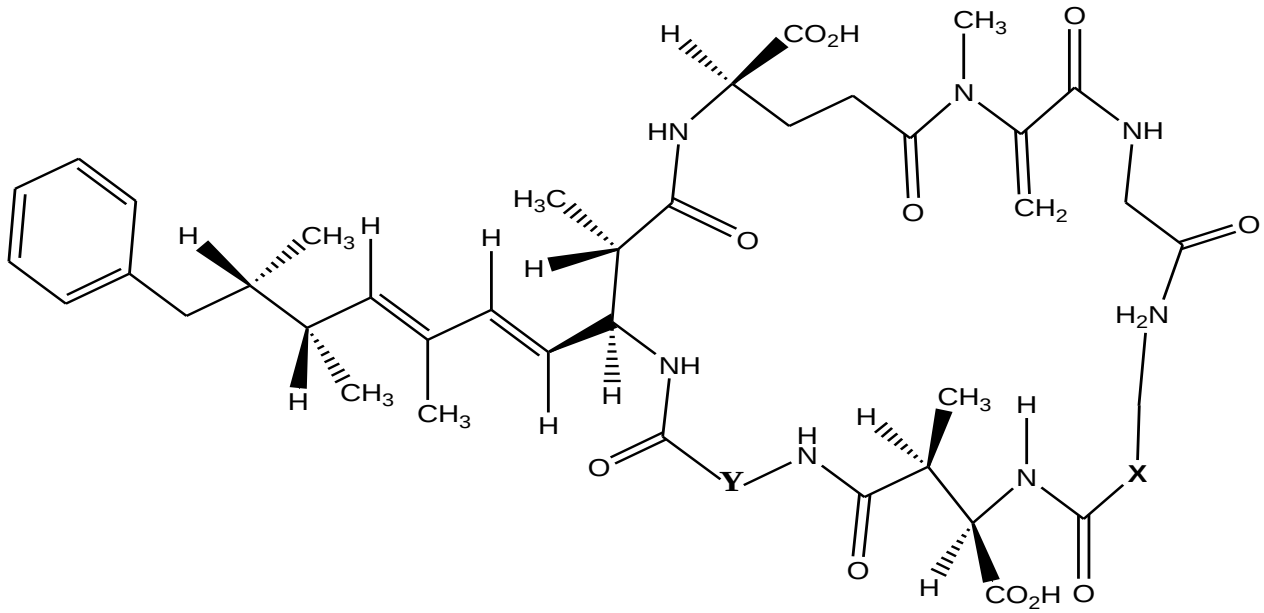

Figure 2.4: General structure of microcystin: The two variable amino acids in microcystin are indicated by X and Y.

The table 1 below gives different microcystin and corresponding two variable amino acids denoted by X and Y, as well as their molecular weight.

Table 1: Variable amino acids denoted by X and Y.

Name	**X**	**Y**	**Molecular weight**
Microcystin-RR	Arginine (R)	Arginine (R)	1038.2
Microcystin -YR	Tyrosine (Y)	Arginine (R)	1045.19
Microcystin -LR	Leucine (L)	Arginine (R)	995.17
Microcystin -LA	Leucine (L)	Alanine (A)	910.06

Figure 2.5 below illustrates the structure of MC-LR.

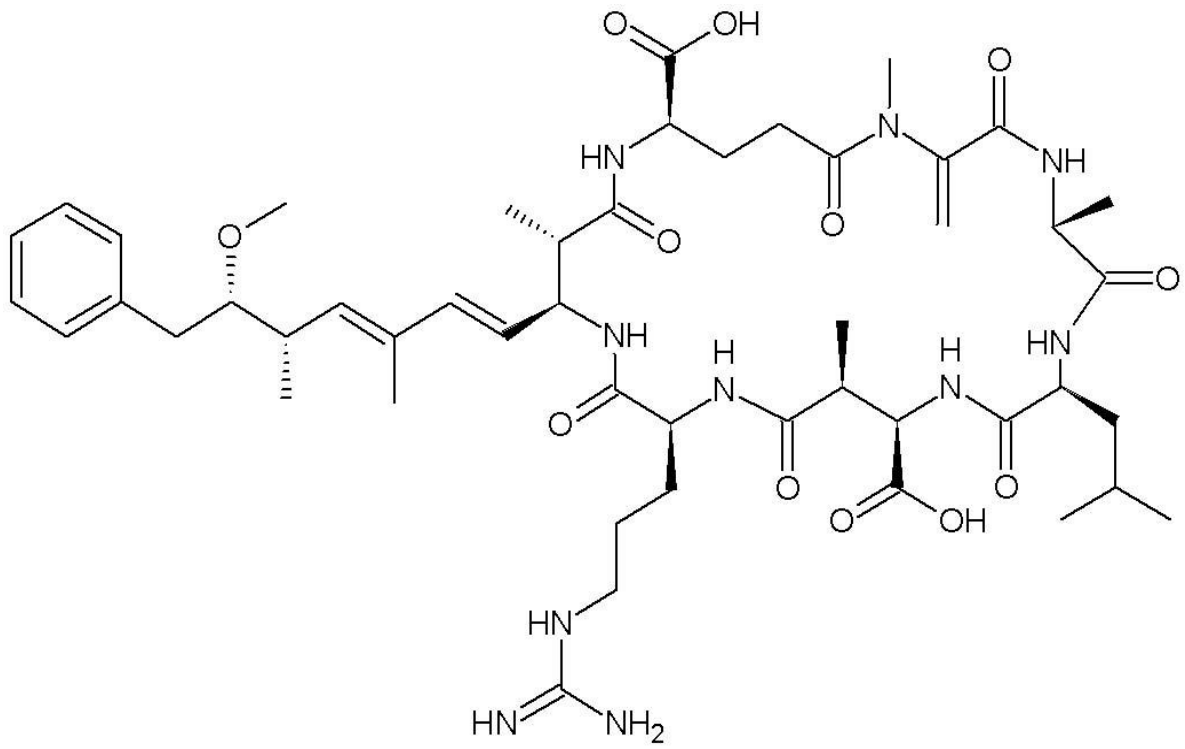

Figure 2.5: Structure of MC-LR.

In addition to their exposure through contaminated water, the MC-LR can also be exposed through the consumption of contaminated freshwater fish, micro-algae dietary supplements and seafood (Ibelings *et al*., 2005; Ortelli *et al*., 2008). The MC-LR is hepatotoxic in nature and mainly targets the liver, promoting the formation of hepatic tumours through chronic ingestion of contaminated food or water. Long term consumption of a large dose can be fatal as the MC-LR may also affect the gastrointestinal tract and the kidney (Azevedo *et al.,* 2002; WHO). The symptoms usually include blurred vision, abdominal pain, headache, vomiting and nausea among others.

Numerous fatal poisonings of wildlife and livestock have been documented by the World Health Organization (WHO). In February 1996, out of 131 patients in Caruaru, 116 experienced nausea, visual disturbances, muscle weakness and vomiting following routine dialysis. Among the 116 affected, 100 developed acute liver failure with 52 eventually dying from the symptoms. This syndrome existed due to cyanotoxins from a water basin that was not treated. Microcystins were present in the water reservoir as well as the livers and blood of the patients.

The incidences of these toxic cyanobacterial algal blooms have become more frequent and present coverage increasing worldwide, thus there is need for their routine as well as accurate detection in drinking and recreational water bodies. The WHO established median lethal dose (LD50) of the MC-LR is 5 mg/kg and the maximum concentration limit in daily drinking water is 1 mg/L (WHO).

Currently technologies used for the detection of Microcystins depends mainly on two methods: analytical methods such as liquid chromatography (LC) or biochemical screening methods like enzyme-linked Immunosorbent assays (ELISA) (Pyo *et al*., 2006;

Lindner *et al.*, 2004), protein phosphatase inhibition assays (PPIA) (Cai*et al.*, 2006) or competitive enzyme immunoassays (Long *et al.*, 2009; Khreich *et al.*, 2009). Analysis of microcystin-LR using HPLC on C-18 following extraction of cells with 75% methanol has achieved a detection limit of 0.1–1mg/litre (Song *et al.*, 2008). A detection limit of 0.1–0.5mg/litre has been achieved using immunoassay kits (ELISA) for Microcystins dissolved in water (Moreira *et al.*, 2014). Protein phosphatase assay detected 0.5–1.5mg/litre Microcystins dissolved in water (Mountfort *et al.*, 2005; Sangolkar *et al*., 2006).

However, all these methods mentioned above have their inherent disadvantages. For example, the LC methods usually require time, consuming sample preparations that involve the pre-concentration of substantial amount of water volumes prior to analysis. The PPIA and ELISA on the other hand might not be able to distinguish between the various Microcystins as well as unrelated protein phosphatase inhibitors (Sangolkar *et al*., 2006). Recently reported are nuclear magnetic resonance and optical measurements (Long *et al*., 2009; Lindner *et al*., 2004). Although offering a high sensitivity, these methods are rather complicated, normally require time consuming sample pre-treatment procedures, highly skilled operators and expensive instrumentation, making them inappropriate for routine monitoring of the microcystin. As an option, different biological and chemical sensors have been reconnoitred for detection of these toxins.

The current work focuses on the sensing of the Microcystins using the BPE-FeNPs based aptamer sensor with cyclic voltammetry as the read out.

2.5 Sensors and Biosensors

A sensor is characterized as an apparatus that measures or detects a physical property then records, shows or responds to it. The three sorts of sensors include; physical sensors,

chemical sensors, and biosensors (So *et al*., 2005). A physical sensor measures physical quantities such as pressure and temperature. A chemical sensor on the other hand responds to an analyte in a particular manner through a synthetic reaction that can be subjective or quantitative.

Electrochemical sensors are a type of chemical sensors in which the electrode is employed as a transduction element. They have been explored significantly in the past years, with the advancement of DNA detection and enzyme biosensors techniques leading the way.

A biosensor device incorporates a biological sensing component that is joined to a transducer. The analyte detected by this instrument might be of biological, inorganic or organic components. Most biosensors consist of specific molecular recognition probes that target an analyte of interest and a means of translating that recognition event into a quantifiable signal. A molecular recognition is the basis of bio sensing and there has been increased attention on the development of novel molecular recognition probes. Antibodies have been the most employed molecular recognition probe for several years and have been integrated into biosensors (Ricci *et al.*, 2007). Despite their specificity and affinity, they are disadvantaged as they are not satisfactorily reproducible, have short shelf-lives and can be challenging to incorporate into the biosensor platform. Many of these disadvantages experienced when using antibodies can be avoided by using a molecular recognition probes of synthetic origin.

The new technologies of aptamers have emerged as viable alternatives for use in biosensors as they have in vitro selection and production (Mascini*et al.*, 2007). This work focused on the aptamers for microcystin targets as well as the incorporation of this probe into the biosensor platform.

2.6 Detection of Microcystins

2.6.1 Immunoassays

Immunochemical methods have been vital for the recognition of Microcystins in open surface water bodies (So *et al.*, 2005). Immunoassay antibodies and kits are available for some cyanotoxins; however, it is difficult to identify the antibodies used. Considering the major impact of these antibodies on measure execution, this is a noteworthy drawback of these test kits. Zeck *et al*. (2001) developed a monoclonal antibody for all Microcystins having an Arginine (R) at position four, including the frequently occurring microcystin-RR and microcystin-LR. A new monoclonal antibody specifically against microcystin-LR has been developed (Fodey *et al*., 2011). Antibodies are still extremely costly and all the efforts to reduce their cost have not been achieved significantly. Therefore, the application of antibodies in detecting microcystin is limited by their cost.

2.6.2 Multiplexed Biosensors/Biosensor Arrays

The multichannel immunosensor based on capillary ELISA technique was published by Lindner *et al*. (2004). The method remained rapid with a detection limit of 0.2 µg/L. Long *et al*., published a paper in 2009, which described fibre-optic biosensors for the detection of various analytes, like microcystin-LR and TNT.

However, the use of antibodies in developing biosensor is limited by temperature and pH sensitivity, easy degradation and short shelf life.

2.6.3 Aptamers

Aptamers are synthetically made oligonucleotides that are generated to selectively bind to inorganic or organic substrates as well as low molecular weight macromolecules such as proteins and drugs (Zhao *et al.*, 1999). Aptamers has various property advantages compared

to antibodies such as broader target choice, high affinity, long term stability and high thermal resistance. In addition they are relatively cheap, easy to produce and modify, and have no batch to batch variations (Niazi *et al.*, 2008). Therefore, it is not surprising that aptamers are currently being widely employed in biosensing applications.

Figure 2.6 shows the MC-LR binding aptamer in secondary fold determined by mfold software.

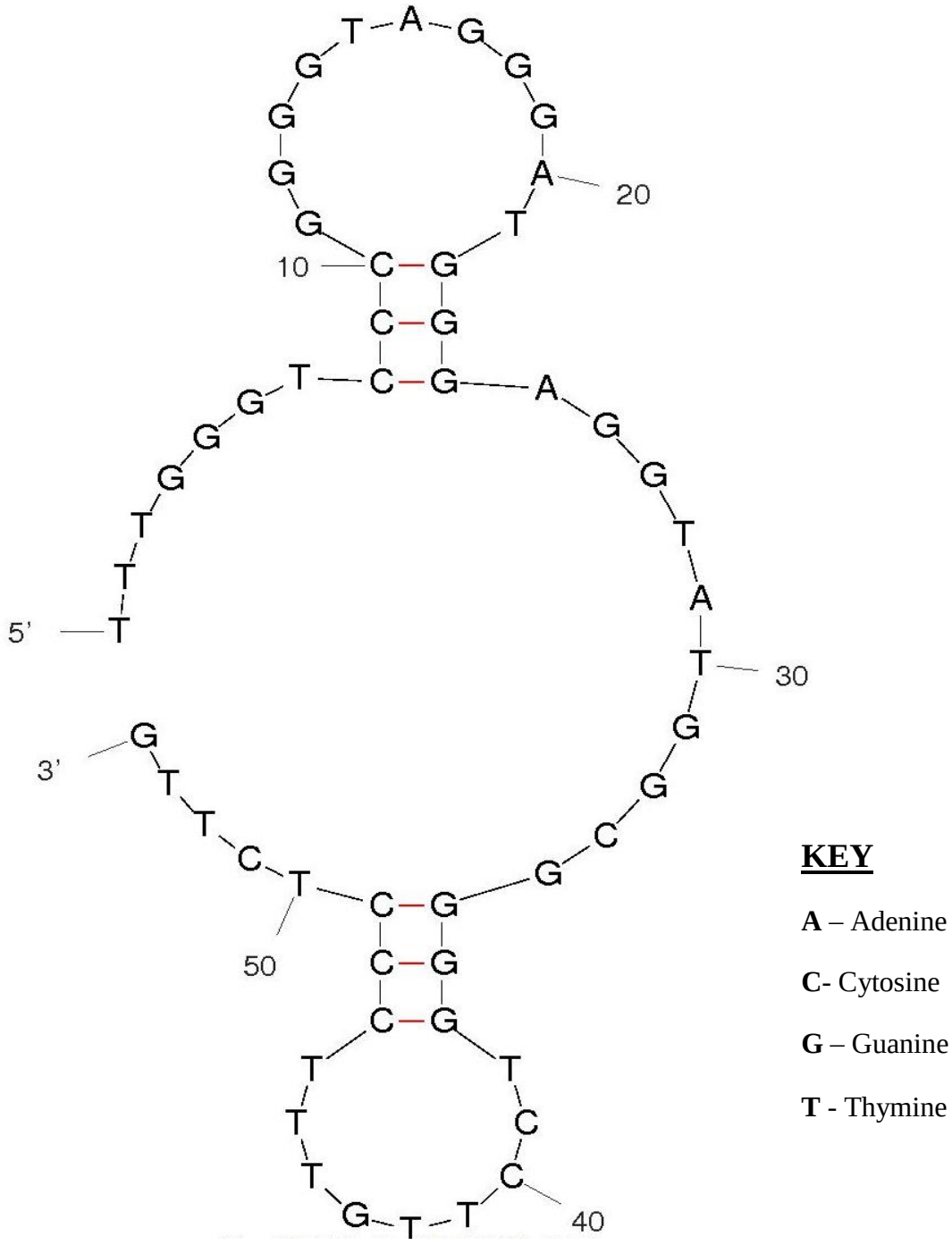

Figure 2.6: The MC-LR sequence for the MC-LR-binding aptamer in secondary fold determined by mfold software.

The advantages the aptamers have over antibodies include (i) Chemical modification of the aptamers with functional groups to enable them tether to the detectors is much easier than with antibodies (ii) no need for Ag: Ab complex since the adjustment of aptamer with a name is possible as well as direct analysis of aptamer to substrate interaction and (iii) The synthesised aptamers are highly reproducible compared to antibodies. Aptamers offer a helpful contrasting option to antibodies as sensing molecules and has given advancement in biosensing (Song *et al*., 2008).

A label free aptamer based sensor for detection of low weight molecules has been reported (So *et al.,* 2005). Aptasensors have demonstrated that aptamers can substitute antibodies in biosensing. This study was aimed at developing Fe nanoparticle based aptamer sensor for the detection of microcystin-LR.

Scheme 2.3 demonstrates sensing mechanism for microcystin using microcystin binding aptamer (MB) functionalized gold electrode.

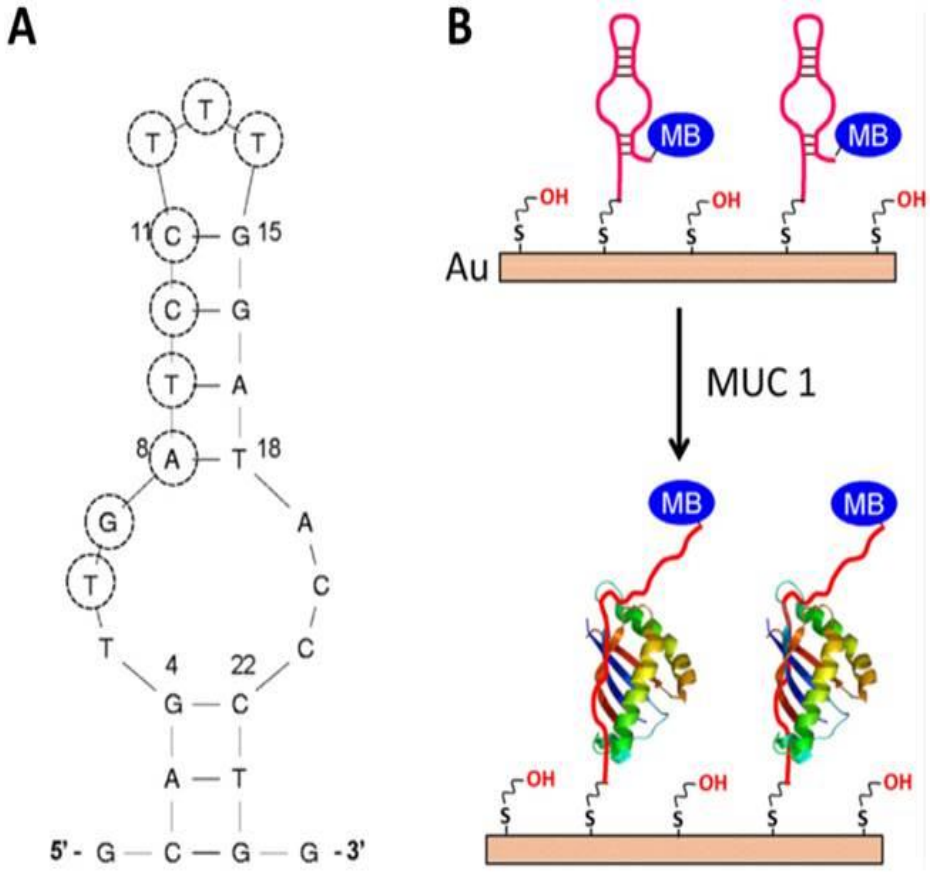

Scheme 2.3: Schematic representation of sensing mechanism for microcystin using microcystin binding aptamer (MB) functionalized gold electrode.

2.6.4 Systematic Evolution of Ligands by Exponential Enrichment (SELEX)

SELEX is an *in vitro* process developed over past few years for selecting different nucleic acid sequences from a pool of DNA or sometimes even RNA for targets ranging from proteins to small molecules (Gopinath, 2007; Stoltenburg *et al.*, 2007). The general SELEX procedure starts with an initial 10^{14} - 10^{15} pool of nucleic acid sequences of either RNA or

DNA. SELEX libraries of RNA or DNA are made up of nucleotide positions flanked through primer binding sites for signal amplification. The selected pool is incubated together with the target molecules subjected to several washing steps and then eluded of the binding sequences before being amplified through polymerase chain reaction (PCR). The elution step is important since it ensures that the desired aptamer is completely isolated (Berezovski *et al*., 2006).

The most fundamental part of the SELEX procedure is ensuring selection of aptamers with high specificity and affinity through efficient separation of nonbinding and target binding oligonucleotides. This process shows the strength of a molecular interaction with the target aptamer under given environmental factors like pH and ionic strength. SELEX procedures usually require 6 − 20 rounds of selection so as to get high-affinity aptamers. After the selection procedure, the enriched pool of aptamer is cloned, sequenced and characterized with the desired properties before being synthesised chemically in large quantities.

Aptamers obtained through the SELEX (Figure 2.7) procedure bind specifically and highly with the target molecules or cells (Ellington, 1994). The Aptamers also have the ability to differentiate one cell type from several other cell types. This discrimination capability revealed during the SELEX method has been developed recently for production as well as selection of aptamer molecules. The success of the SELEX procedure depends on the libraries of random oligonucleotides that can allow quick screening. Combinatorial chemistry techniques is currently being used as it allows fair cost and straight forward production of random sequence oligonucleotides through repeated duplication of the natural 30–50 linkage (Fang and Tan, 2009).

Figure 2.7 Showing SELEX procedures for selecting aptamers against a specific target.

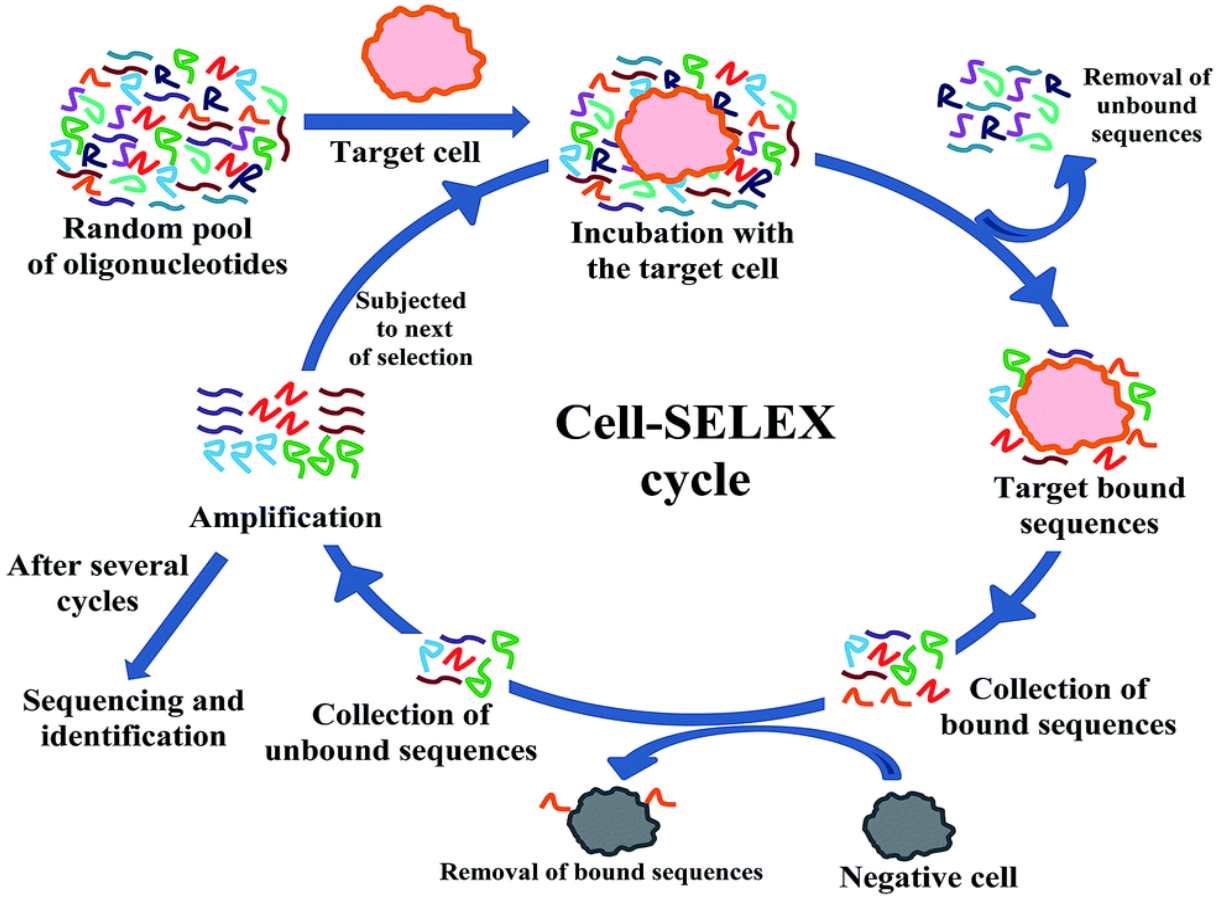

Figure 2.7: SELEX procedure for selecting aptamers against a specific target.

2.6.5 Electrochemical redox detection.

Electrochemistry is commonly used in aptamer sensors readout. Ochratoxin A (OTA) was detected sensitively using it (Eissa *et al.*, 2014). As of late, electrochemistry has been utilized for more prominent sign enhancement in aptasensor for thrombin (Yigit *et al.*, 2008).

2.6.6 Chemiluminescence detection

It is a readout technique that is broadly used in aptasensors. (Lu *et al*) used diverse enzymes and this method to identify adenosine and cocaine simultaneously. Here, introduction of the target reduces the amount of the binding enzyme leading to reduced chemiluminescence which is then used as the readout signal in the aptasensor. Aptamer sensors employing

chemiluminescence detection have had broad applications in diagnosing several genetic related diseases.

2.6.7 Detection via personal glucose meters

This technique was technologically advanced by Zhang *et al.* (2011) to quantify numerous compounds such as adenosine, cocaine, uranium and tuberculosis. These sensors used multiple aptamers with detection based on existing personal glucose. The assays could generally be applied to any molecular target with known aptamers and were suited for home diagnosis. Their sensitivity which was approximately between nanomolar for proteins and micro molar for small molecules was however yet to be compared to those of clinical assays.

2.6.8 Fluorescence detection

Zhao *et al.* (1999) manipulated the enzymatic activities of protein targets for their enhanced sensitive detections. They used numerous aptamers to productively capture the targeted protein. It was then washed to remove excess species and before a fluorigenic substrate which is specific for the catalysis added. This formed many fluorescent products for sensitive recognition of target proteins with detection limits of 100 fM being achieved. This type of sensing technique is however limited since it can only be employed for targets with enzymatic activities.

Another fluorescence based detection employing the use of fluorophore labelled aptamer for detection has also been developed (Zhang *et al.*, 2011). In this situation, the binding of the target to the aptamer displaces the conjugate aptamer resulting into increased fluorescence intensity.

A sensitivity of 170 µM of this method is however lower as compared to other ultrasensitive approaches described above. Nevertheless, fluorescence-based sensing technique has been used to concurrently detect thrombin and lysozyme.

2.6.9 Electrochemiluminescence (ECL) detection

ECL is a considerable sensitive readout technique that has been exploited by Herr and the group (2006) for cancer cells detection. Nano probes of Au–CdS or Au-CuS was utilised for enhancement of the ECL signal and the sensor gave impressive sensitivities for a DNA sequence target with a detection limit of 6.8 µM being achieved.

2.6.10 Surface plasmon resonance

Wang and co-workers (2009) described an alternative format for aptamers that uses surface plasmon resonance (SPR) biosensor having an amplified effect of Gold nanoparticles (AuNPs). The platform was used to recognise adenosine via surface inhibition detection. The adenosine aptamer was initially immobilized on a SPR gold film before being hybridized with ss-DNA labelled with AuNPs. This resulted into change in the SPR signal with the adenosine aptamer adopting a tertiary structure after adding adenosine to the SPR cell. The tertiary structure could not hybridize with tagged ss-DNA and this led to decreased SPR signal that is proportional to the small molecule concentration.

2.7 Applications of aptamers

Aptamer assays that uses adenosine triphosphate (ATP) as the target compound to detect small molecules was adopted by Deng *et al.* (2003). Several of these biosensors employ structure switching design in which the target aptamer first forms a duplex structure before the structure is broken by the introduction and binding of target. This technique has been used in electrochemical biosensors with similar approach to also detect lysozyme. The

sensitivity of some of these assays has been upgraded through labelling the aptamers with nanoparticles such as those of gold.

Song *et al.* (2008) described an application of aptamers with detection platform technologies for developing assays capable of analysing drugs and environmental contaminants. The constructed label free electrochemical aptasensor was used for detection of cocaine and female steroid hormone.

Fluorescence based displacement has been employed for detection of mycotoxin concentrations although the method was not sensitive enough.

Niazi *et al.* (2008) have developed five aptamers for the antibiotic oxytetracycline (OTC) and neomycin B. The SPR based biosensor assays were immobilized onto gold sensor surface and the measurable response resulting from the interaction with aptamer recorded.

An RNA-aptamer based assay for detecting MG and leucomalachite in fish has also been developed. The assay is capable of sensing MG residues in 2lg/kg test samples and has high tolerance to different solvents (Zhao *et al.,* 2012).The binding capacities of lipocalin odorant binding protein for detection of low molecular weight explosives such as diphenylamine, dinitrotoluene and dimethylphthalate have also been investigated (Kim *et al.*, 2007). The authors indicated that odorant binding protein could indeed be used as a biosensor for sensing explosives.

2.8 Polyaniline (PANI)

To enhance the sensitivity of the aptasensors, they are often tailored together with conducting polymers, solid electrolytes, semiconductors, metals, insulators, catalytic materials and nanomaterials (Zhao *et al.*, 1999). Some of the materials that have been employed in aptasensors include polyaniline (PANI), carbon nanotubes (CNTs) and dendrimers. The

process of incorporating novel materials into transducers has enhanced the electrochemical aptasensor response (Horiuchi and Nakao *et al.,* 2007). The solid incorporation of nanomaterials into bulk matrix of polymers is known as a nanocomposite and entails the integration of metal nanoparticles into a matrix of a polymer (Bose *et al*., 2010).The polymer nanocomposite has special properties which cannot be found within a single material (Speets *et al.,* 2005).

These properties of polymer nanocomposites have led to applications of these materials in various fields such as in biosensors, high charge density batteries, photovoltaic devices and colloid stability (Jeong *et al*., 2004).

Conductive polymer mechanical strength, thermal and electrical conductivity are drastically enhanced by incorporating metal nanoparticles (Vincent, 1995).The metal nanoparticles surfaces have interfacial properties that form self-assembled monolayer with organic functional groups within the polymer yielding sensing interfaces in a variety of aptasensor platforms (Jeong *et al*., 2004). Therefore, aptamer conjugated polymer nanocomposites offer a powerful means of target recognition in aptasensor development.

Possible applications of conductive polymers include super capacitors and electrolytic type capacitors. Their valuable electronic properties, light weight, mechanically flexible and cost effective enable their incorporation into various functionalities in their matrix during or after polymerization. In addition, by monitoring the polymerization charge during sensor fabrication, the viscosity of the recognizing film can be measured (Spinks *et al.*, 2002; Riley and Wallace, 1991).

Polyaniline (PANI) and its derivative is a standout amongst the most useful conducting polymer **(Figure 2.8)** with numerous applications like in organic light emitting diodes, field effect transistors, sensors, corrosion and solar cells ((De souza , 2007; Jeong *et al*., 2004).

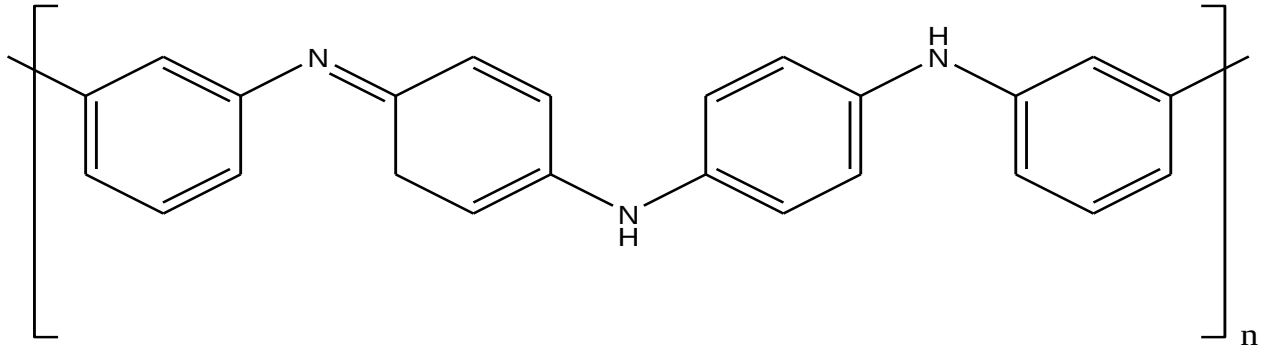

A

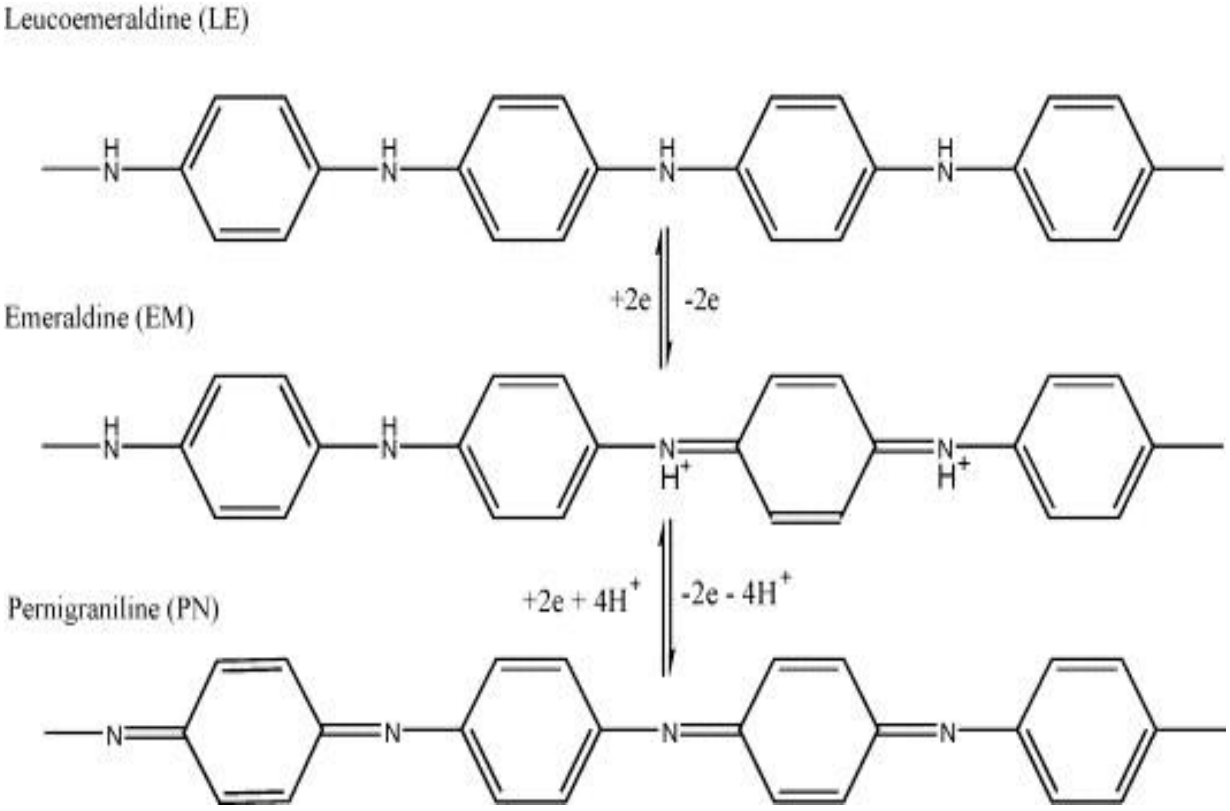

B

Figure 2.8: A; Structure of PANI and B; PANI redox states.

In this study, PANI was electrochemically incorporated into the sensor system and employed to enhance the sensitivity of the aptasensor as well as serve as a support material for the attachment of the iron nanoparticles.

2.9 Analytical techniques for the characterization of FeNPs

2.9.1 XRD technique

X-ray diffraction techniques are analytical procedures which give data about the crystal structure, physical properties and synthetic composition of materials (Treacy and Higgins, 2007). It is a standout amongst the most useful characterization techniques in material and solid state science. X-rays are produced when high energy particles such as electrons are accelerated through a given voltage and then collide with a target, for example, Iron. The electrons have adequate energy that can ionize some of the inner K-shell electrons of Fe. This result into electrons from the outer orbital immediately drops down to occupy the now vacant inner orbital. X-rays are released during these transitions in form of energies with fixed values. The energies are material dependent, which implies that each material has its own characteristic X-rays patterns. This characteristic X-ray pattern can be utilised as a "fingerprint" for identification of different materials. The powder patterns of most known solids are contained in the Powder Diffraction File.

The electron beam used in production of X-rays is provided by a heated tungsten filament. The beam is accelerated through a potential difference of several kV towards an anode. The X-ray tube is evacuated so as to prevent oxidation of the filament and the produced X-rays leave the X-ray tube via the windows.

When a monochromatic X-rays beam strikes a powdered sample that has crystals randomly arranged in every orientation, with some crystals oriented at Bragg angle, diffraction occurs.

The diffracted beam is then detected by a movable detector or a photographic film. XRD analysis can be completed on different types of samples, however, the perfect sample is a crystalline powder squeezed into the specimen holder. The sample should also have a smooth surface and held at an angle of 45 degrees in the sample holder. Small volumes of solid sample taped on a microscope slide glass or a thin film deposited on a substrate may likewise be used. Better results are achieved with crystalline sample.

At the point when X-ray radiation with a wavelength λ is directed on a material, a diffraction peak is observed when the Bragg equation is fulfilled:

$$n\lambda = 2\mathrm{d}\sin\theta$$

Where d is the lattice space of the material, θ the incidence angle, λ is the Cu Kα emission wavelength and is equal to 1.5418A°. A powder XRD pattern can also be used to determine the size of the nanoparticles using the Scherrer formula:

$$L = 0.9\lambda$$

Where L is the particle size and λ is the Cu Kα emission wavelength (1.5418A°.)

This technique was utilised to determine crystallinity of BPE synthesised Iron nanoparticles. The analysis was conducted using a diffractometer operated at 45 KV within Cu Kσ radiation and a graphite monochromator that produces x-rays with a wavelength of 1.54060A°.

2.9.2 Transmission electron microscopy (TEM)

TEM device is used for size characterization of nanoparticles and when aligned well and stable with a fixed magnification can allow a great number of the nanoparticles to be seen within the micrograph. This microscopic technique uses an electron beam which is conducted over a thin sample and producing an interaction as it passes through the specimen (Williams and Carter, 1996). They are hastened through a high voltage and speed that is approaching

that of light. The associated wavelength of these electrons are five times smaller than the light wavelength (0.04-0.008 Å).The image formed by the interaction is magnified and directed to an imaging gadget, such as a photographic film, fluorescent screen or a sensor like a charge coupled gadget camera.

The ideal sample for TEM nanoparticle size analysis should have large number of the nanoparticles occupying the desired micrograph field of view. In addition, the nanoparticles should be without excessive bunching or agglomeration. The specimen used in the TEM grid has to be very thin (0.1 to 10mm) to allow electrons penetrate and thereby form images.

TEM resolution to the order of Å enables specimen imaging as well as structure elucidation at the atomic level. Conventional transmission electron microscope uses the transmitted beams and some of the forward scattered beams in creating a diffraction image which can either be in dark or bright field mode. The bright field image results from the directly transmitted beam only while the dark field image is as a result of collected scattered electrons.

In the present study, transmission electron microscope was employed in the characterization of the biosynthesized Fe nanoparticles.

2.9.3 Energy Dispersive X-Ray Spectroscopy (EDXS)

The signal here is typically among the several diverse types of signals delivered from a specimen surface under an electron beam. It results from the recombination interactions of free electrons with positive electron openings created inside a specimen. The x-ray signals enable the determination of elemental composition using the EDXS analysis of the characteristic x-ray signals.

EDXS is currently quasi systematically incorporated into transmission electron microscope instruments thus constituting a powerful set known as analytical electron microscopy (AEM) (Yau, 1987). EDXS is a quick technique for qualitative and quantitative analysis of materials. In this work, EDXS coupled to transmission electron microscope instrument was utilized to identify the elemental composition of the biosynthesized Fe nanoparticles.

2.9.4 Scanning electron microscopy (SEM)

SEM is a microscopic technique which takes images of a specimen by scanning it using high energetic electron beam. The electrons interact with the specimen atoms producing signals containing data of specimen's surface composition, topography and electrical conductivity. In SEM, electrically non conducting specimens are covered with a thin conducting film such as of a metal or carbon (Duke, 1990).

SEM instrument is composed of two principle components; the electron column and the electronic console. The electronic console contains switches and control knobs for adjusting instrument’s filament current, focus, magnification, accelerating voltage, contrast and brightness. Some of the modern electron microscopes uses electronic console in conjunction with the computer systems thus no need for bulky console for housing control knobs and switches. In such SEM instruments, all the primary controls are available through the mouse and keyboard of the computer system. The electron column consists of the electron beam that is produced under a vacuum and focused through a small diameter so as to scan across the specimen surface. The lower part of the column is known as the specimen chamber and houses the secondary electron detector. SEM samples are mounted onto the stage that is controlled by a goniometer.

In scanning electron microscopy, two types of signals are used for the visual examination of the material surface; secondary and backscattered electrons. Secondary and backscattered electrons are continuously created from the specimen surface under electronic beam, though they result from two different types of interaction. Figure 2.9 below shows a schematic diagram of different radiations produced during interaction of a material with an electron beam.

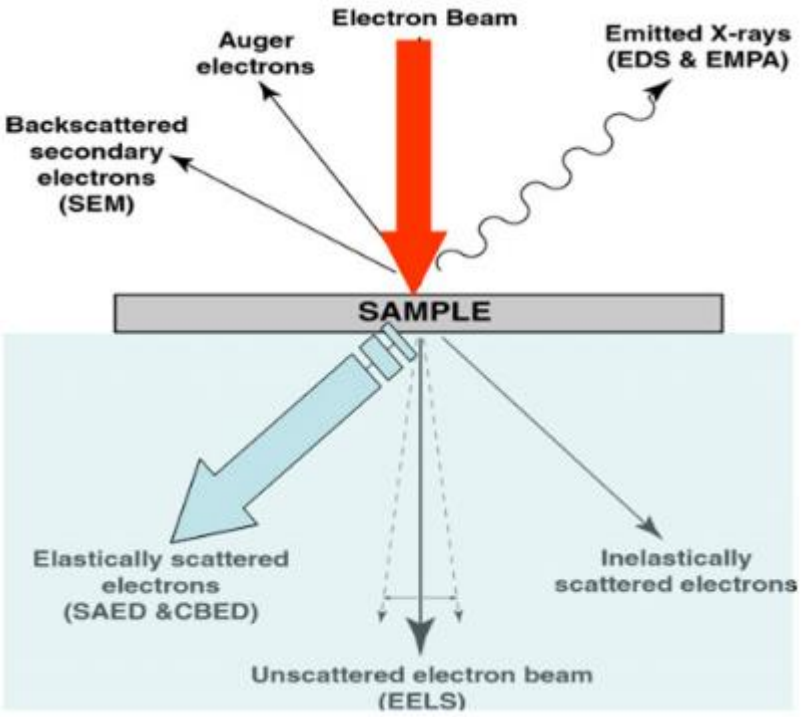

Figure 2.9: Schematic diagram showing different radiations produced during interaction of a material with an electron beam.

As can be seen from **figure 2.9**, secondary electrons result from the inelastic collision followed by scattering of the incident electrons with the electrons of the specimen. These electrons are characterized by energies less than 50 eV and used to study the surface structure of the specimen with a resolution of approximately 10nm or better (Watt, 1985). Backscattered electrons result from the elastic collision and scattering interaction between

the incident electrons and nuclei or electrons of the specimen. They can be produced further from the specimen surface and reveals the topographical contrast as well as the atomic number contrast.

2.9.5 Ultraviolet-visible spectroscopy (Uv-Vis)

This is a spectroscopic technique that makes use of the ultraviolet and visible spectral regions. of Ultraviolet (UV) and visible radiations are absorbed by particles accompanied by excitation of their electrons from lower to higher energy levels. Most molecules undergoing electronic excitation have to absorb light, though, some molecules require more energetic radiations (in the vacuum ultraviolet, <200 nm). A molecule has to contain either non-bonding orbital or valence bonds for it to absorb radiations in the UV-Vis regions (200 – 800).

When UV-Vis radiation passes through a material, part of it is absorbed by the material, causing the outer electrons to be moved from ground energy state to excited energy state. Normally, the electrons move from a molecular orbital. Detectors like photocell are then used to detect the radiations that have been transmitted. The amount of radiation absorbed is usually expressed as either transmittance or absorbance. A plot of the degree of absorption against the wavelength of incident radiation is then recorded on the read out meter.

To obtain a spectrum, the absorption of radiation by the sample is measured at various wavelengths. Each line in the spectrum represents the wavelength at which the energy of the incident radiation equals the energy required to effect a transition. Presence of an absorption band at a given wavelength indicates presence of a chromophore and its position depends on the chemical environment of the sample. Parameters like the pH, temperature, and concentration cause changes both in the intensity of the absorption maxima and wavelength.

2.9.6 Fourier Transform Infra-Red spectroscopy (FTIR)

Fourier transform infrared spectroscopy allows detection of infrared (IR) absorption as well reflection properties for a wide spectral region (Bell, 2012). This type of spectroscopy consists of a Michelson interferometer that has a beam splitter, a moving mirror and a fixed mirror as shown in figure 2.10.

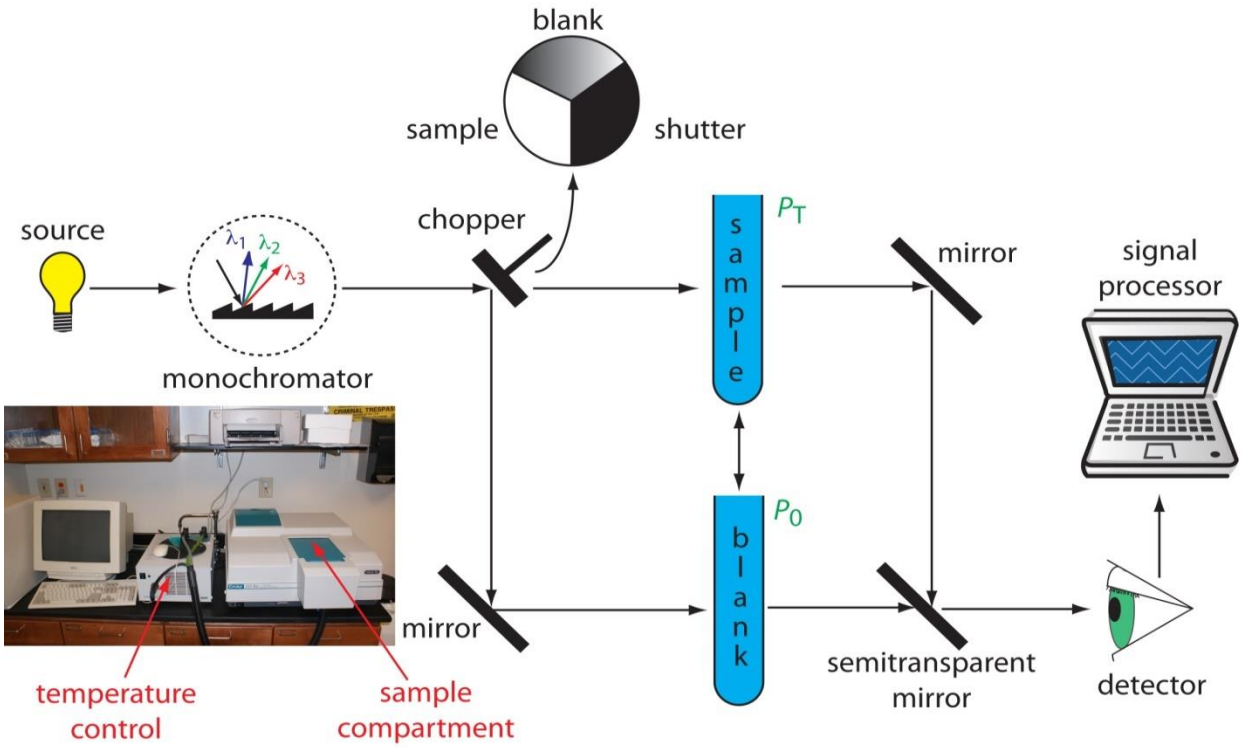

Figure 2.10: Schematic diagram of FTIR.

In FTIR spectrometer, the data across the wavelengths in the spectrum is recorded concurrently. Throughout every scan, it registers a shorter time scan compared to a dispersive spectrometer. In dispersive spectrometer energy throughput is usually restricted by the exit and entrance slits of the monochromator. In the FTIR, no slits are required and thus higher intensities measurements are possible (Griffiths, 1975). The FTIR frequency range depends on the source of light, detector and beam splitter employed. Commonly used beam splitter

includes thin films deposited on non-absorbing substrate and Mylar thin films. Infrared detectors are either quantum or thermal in nature.

Attenuated Total Reflectance (ATR) is currently the greatest broadly employed FTIR sampling apparatus that allows quantitative or qualitative analysis of samples with no or little sample preparation. It has led to rapid and fast sample analyses with extremely thin sampling path length or IR beam depth of penetration. ATR technique is better than the traditional FTIR sampling techniques in which the sample had to be mixed with salt before pressing it into a thin film preceding analysis. This was done to avert the totally absorbing bands from appearing in the infrared continuum. In ATR sampling, an IR beam directed into a crystal with relatively higher refractive index is reflected from the internal surface of the crystal, creating an evanescent wave. This wave is then projected orthogonally to the sample which is in an intimate contact with the attenuated total reflectance crystal. The sample absorbs some of the energy of the evanescent wave and reflects some which then is returned to the detector (Rabolt *et al.*, 1983). Figure 2.11 shows attenuated total reflectance.

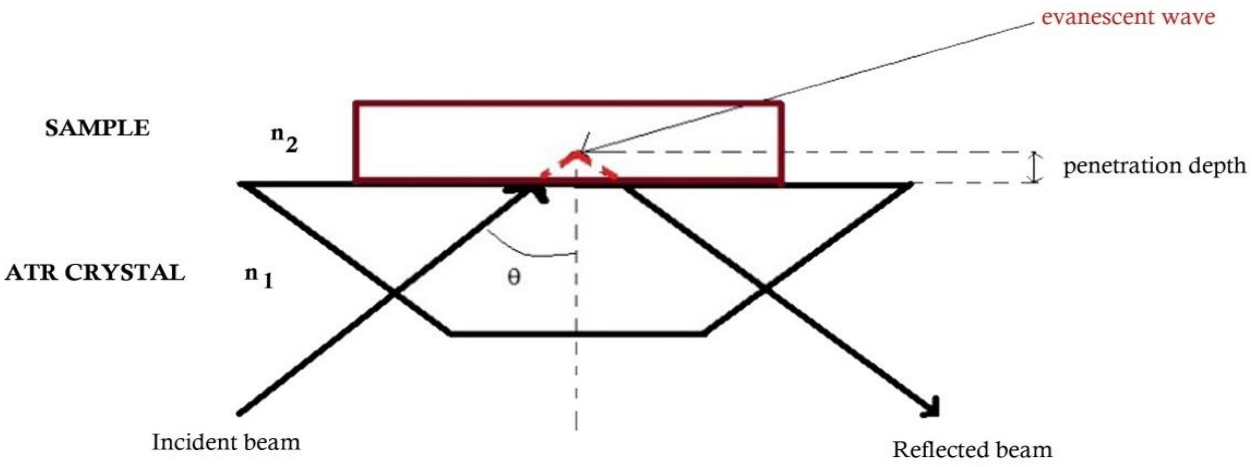

Figure 2.11: Graphical representation of a single reflection in ATR-FTIR.

.

The refractive index of crystals is governed through the equation;

$$\Theta_c = \mathrm{Sin}^{-1}(n_2/n_1)$$

Where n_2 is the sample refractive index, n_1 the ATR crystal refractive index and θ_c is the critical angle. ATR spectral result when the critical angle is exceeded while a combined ATR and external reflectance is observed when the critical angle is not met. When the angle of incidence of the IR beam is too low, the ATR crystal refractive index is also too low, the sample refractive index too high or when there is a combination of these 3 factors, the critical angle is not met and a combined spectral is observed.

2.9.7 Electrochemistry

Electrochemical techniques are versatile and powerful analytical techniques that offer high accuracy and sensitivity. They are also precise, relatively of low cost instrumentation and with large linear dynamic range.

Electrochemical methods are classified as Amperometric and Potentiometric. In potentiometry, the response is kinetically facile and the potential of the cell under conditions of no current flow is measured. The cell potential corresponds to the adjustments in the chemical movement of the species present in the electroanalytical method. In this type of electrochemistry, the controlled parameters which are the potential of the working electrode that vary with time and the current flowing in the working electrode are measured. In amperometry, kinetics of reaction is determined by an applied potential and the diffusion controlled current flowing through the solution/electrode interface is measured.

The combinations of different measured parameters result into numerous electrochemical techniques like cyclic voltammetry, chronoamperometry, pulsed techniques, polarography, linear sweep techniques, and chronopotentiometry, among others.

2.9.7.1 Stripping voltammetry techniques

This is a modern electrochemical method with several many stripping techniques such as anodic stripping voltammetry (ASV), cathodic stripping analysis (CSV), Potentiometric Stripping Analysis (PSA) and Adsorptive Stripping Voltammetry (AdSV). These techniques consist of two steps which are concentration and stripping stages. Analyte is pre-concentrated so as to electro deposit it into the mercury terminal which is then reoxidized and stripped out of the electrode in the second step. The peak current (Ip) is utilised to identify the analyte in the sample (Bard and Faulkner 1980).

2.9.7.2 Pulse Voltammetry

Pulse voltammetry technique includes normal pulse voltammetry (NPV) and differential pulse voltammetry (DPV). These techniques consist of successions of potential pulses of increasing amplitude. The peak current produced is measured at the end of every pulse (Kellner et al., 2011).

2.9.7.3 Square Wave Voltammetry (SWV)

In SWV, a general square wave is superimposed on the base of staircase potential is applied to the working electrode (Bard and Faulkner 1980). Square wave voltammetry response is faster than DPV for irreversible and reversible cases (Uslu and Ozkan, 2002).

2.9.7.4 Cyclic voltammetry

Cyclic voltammetry involves scanning the working electrode potential at a particular scan rate then measuring the subsequent current. Frequently the sweep potential is reversed at a given switching potential. As initial and switching potentials are known, it is easy to convert time to potential and the normal protocol is to measure current against the applied potential.

Current versus applied potential curve is known as cyclic voltammogram and figure 2.12 illustrates the shape of an ideal and reversible system.

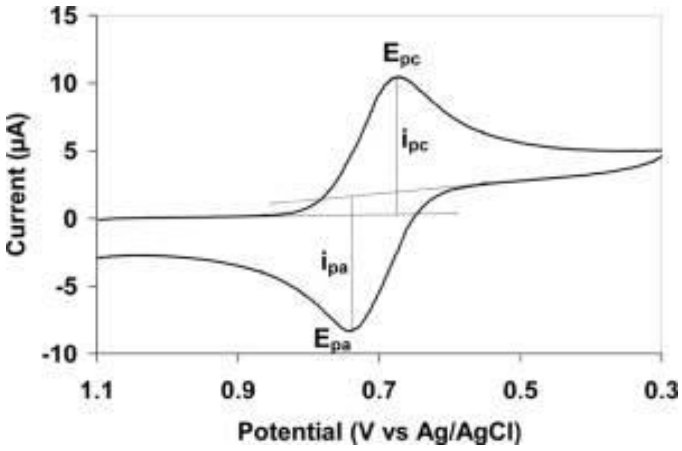

Figure 2.12: cyclic voltammogram.

The most useful parameters in cyclic voltammetry are the peak potentials (E_{pa}, E_{pc}) and the peak currents (i_{pa}, i_{pc}) for the cathodic and the anodic reactions. The peak current (i_{pA}) for anodic oxidation process is the highest current value that results from an oxidation reaction taking place at the electrode surface. The maximum respective potential at this peak current is called the anodic peak potential (E_{pA}). Reversing the potential back to the initial potential results into respective peak cathodic current (i_{pC}) and peak potential (E_{pC}) for the reduction reaction.

The electrochemical oxidation and reduction reactions are considered reversible when the electron transfer process is fast in either direction and both the cathodic and anodic waves are well defined. In addition, the positions of peak potentials should not change with change in potential scan rate.

Information can be drawn from the reactions at the electrode surface even for a single CV voltammogram, though much information can be obtained from multiple CV voltammograms.

CHAPTER THREE

EXPERIMENTAL

3.1 Chemicals and other requirements

Iron (III) chloride was acquired from Merck and was utilised without further decontamination. The ultra-purified and distilled de-ionized water (DDW) were obtained from the Biochemistry laboratory at the University of Nairobi. Banana peels were collected locally from the dumping sites in Nairobi. Microcystin target aptamer were isolated by SELEX process from a random ss-DNA library by Kim et al. (2007). Microcystin-LR was bought from Enzo Life Sciences, USA and was dissolved into 50 mM Tris (hydroxymethylaminomethane), pH 7.5, (150mM NaCl, 2mM $MgCl_2$) binding buffer. This stock solution was further diluted to the required concentrations during the experiments.

3.2 Preparation of aqueous Banana Peels Extract (BPE)

About 100g of fresh taxonomically authenticated peels of banana were gathered, washed exhaustively with distilled water and cut into fine pieces then vacuum dried.

The dry banana peels powder (8.3g) was extracted with 125 ml of DDW at 25, 50, and 80°C while being stirred for 30 min. The concentrate was allowed to cool before being filtered. After extraction, the samples were centrifuged at 8000 rpm for 30 min. The supernatant was collected, filtered and stored at -20°C preceding usage (Njagi et al., 2011).

3.3 Biosynthesis of Iron Nanoparticles (FeNPs) using BPE

Using 0.1 M $FeCl_3$ solution and aqueous Banana peels extracts (supernatant at ambient temperature) in a 2:1 volume ratio, iron nanoparticles were prepared. The mixture was then hand shaken for 1 minute and allowed to stand at room temperature for 1hour. After 10 minutes, the change in colour of the solution from brown to black was noted and recorded.

The mixture was centrifuged at 8000 rpm for 30 min and the supernatant poured out. The black paste obtained was re dispersed in ethanol followed by ultra-purified water to remove excess biological molecules. The process of centrifugation and re dispersion in ethanol and ultra-purified water was repeated 3 times to completely purify the nanoparticles. The light black paste collected was then oven dried at 60^{o}C overnight, packed and stored for characterization (Njagi et al., 2011).

3.4 Characterization and Analysis of the biosynthesised iron Nanoparticles (BPE-FeNPs)

3.4.1 XRD analysis

Crystalline metallic Iron nanoparticles were examined by PAN analytical Xpert Pro θ-2θ powder X-ray diffractometer. The instrument used a Cu Kα radiation at 45 kV with a monochromatic filter in the range of 20-80 degrees. The biosynthesized FeNPs were thoroughly dried to powder form before being stacked in the cubes of XRD equipment.

3.4.2 UV-Vis analysis

Visual observations of the changes in the reaction mixtures were recorded. This was followed with a UV-VIS spectrophotometric examination using a Nicolet Evolution 100 (Thermo Electron Cooperation, UK) UV-Vis spectrometer. The wavelength was scanned from 200 to 700 nm at 1 nm. The instrument was switched on and allowed to initialize for ten minutes. The sample solutions were put in a Quartz cuvette (1cm) and the baseline corrected using ultra-purified water as the blank before carrying out a new experiment. The spectra of BPE extract, Fe nanoparticles and Ferric chloride solutions were obtained in the wavelength range of 200 and 700nm (Njagi et al., 2011).

3.4.3 FTIR analysis

FTIR measurements were done using a Nicolet Magna-IR system 560 with a resolution of 4 cm^{-1}. FTIR scans of iron nanoparticles and BPE extract were taken in order to determine BPE functional groups that may have taken part in the synthesis of iron microstructures. FTIR analysis was carried out in the transmission mode range of 400-4000cm^{-1}.

3.4.4 Scanning Electron Microscope analysis (SEM)

The morphologies of the BPE-Fe nanoparticles were examined using a Hitachi S3000N SEM analyzer with acceleration voltage of 25kV and a resolution 20µm. The BPE-FeNPs samples that were previously dried were put onto adhesive carbon tapes supported on metallic disks and their images were recorded at different magnifications using the secondary electron (SE) mode. All samples were analysed in triplicates and the micrographs recorded.

3.4.5 Transmission electron microscopy (TEM)

TEM made of energy dispersive x-ray (EDX) was used to analyse the morphology of BPE synthesised Fe nanoparticles. The TEM images were obtained using a Philips CM20T-LaB6 TEM microscope operating at acceleration voltage of 120 keV. The Fe nanoparticles sample solutions were sonicated in analytical grade methanol for 20s before being mounted on 200 mesh carbon-coated copper grid. The treated grid was placed face up onto the cleaned Teflon block and 10µL of the nanoparticle sample solution dropped onto the grid and dried under an infra-red lamp prior to grid being loaded onto the microscope for measurements. FeNPs samples randomly chosen from the TEM images were used to calculate and record the average particle size.

Elemental analysis of samples were performed using EDS and its spectra were obtained for 10 µL of Fe nanoparticles placed on a carbon-coated copper grid, measured using an

accelerating voltage of 10 kV. The micrographs and chemical analyses obtained were recorded in a computer.

3.4.6 Cyclic voltammetry (CV)

Basi Epsilon –Ec-ver.2.00.71_XP work station equipped with three-electrode system from Bio Analytical systems, BAS, US, was used to carry out the cyclic voltammetry experiments. A glassy carbon electrode of 3mm diameter and area of 0.071 cm^2 was utilized as the working electrode. Pt wire was used as the auxiliary electrode while the reference electrode was Ag/AgCl electrode. Alumina slurries of 1.0, 0.3 and 0.05 µm and micro polishing pads were obtained from Buehler, IL, USA and employed in the cleaning and polishing of the GCE. All the cell solutions used were bubbled prior to each experiment with analytical grade argon so to degas them. All the experiments were performed at room temperature and pressure and the resulting voltammograms recorded in a computer interfaced to the Basi Epsilon workstation. All the solutions used for the cyclic voltammetry were kept in a refrigerator at -20 ºC when not in use.

3.4.6.1 Pre-treatment of Glassy Carbon Electrode (GCE)

GCE was successively polished on aqueous 1.0, 0.3, and 0.05 µm Al_2O_3 slurries, followed by rinsing thoroughly with ultra-purified water until a mirror like surface was obtained. Then it was washed ultrasonically in absolute ethanol and ultra-purified water each for 5min. Finally, the GCE was air dried at room temperature. All these were done in order to remove the residual polishing material.

3.4.6.2 Immobilisation of nanocomposite film

Electro polymerization of PANI onto the bare GCE was achieved by the use of aniline and ammonium hydrate salt in 97% hydrochloric acid. The potential was swept between -200mV

and 900mV. The formed electrode PANI/GCE was then drop coated using 10µL of synthesized iron nanoparticles before rinsing with ultra-purified water and vacuum drying giving an electrode which was referred to as FeNPs/PANI/GCE.

3.4.6.3 Immobilization of the aptamer onto GCE modified surface

The self-assembly of microcystin targeting aptamer onto the PANI/FeNPs/ modified GCE was prepared as follows: the aptamer was denatured through heating at 90^{o}C for 15 minutes, quickly cooled at 5 ^{o}C for 10 minutes and incubated at 4 ^{o}C for 4 min so as to allow renaturation and attainment of the most stable conformation. For the aptamer immobilisation, PANI/FeNPs modified GCE was kept in a solution containing the microcystin targeting aptamer for 16 hours at 5^{o}C. Finally, the PANI/FeNPs/aptamer was rinsed with ultra-purified water to remove unbound aptamers, followed by air drying. The resulting electrode was then employed as the aptasensor for detecting microcystin.

CHAPTER FOUR

RESULTS AND DISCUSSION

4.1 Visual inspection of the formation of the Iron nanoparticles

The figure 4.1 below shows $FeCl_3$ solution and banana peels aqueous extract solution used in the synthesis of the iron nanoparticles.

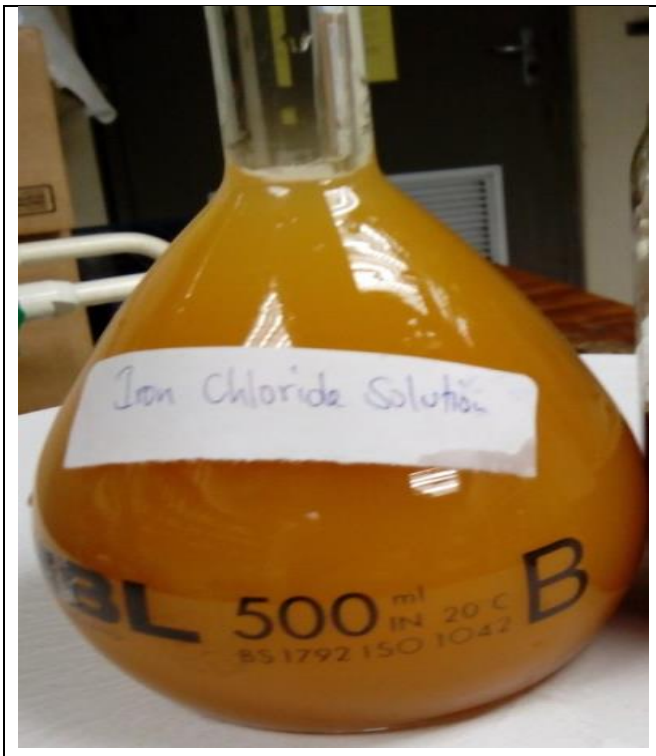

A

B

Figure 4.1: Precursors used in the synthesis of FeNPs; $FeCl_3$ (A) and Banana peels (B).

The colour of the mixture gradually changed from transparent yellow to black in 4 minutes at 90 °C demonstrating the synthesis of iron nanoparticles (figure 4.2). The dark colour was as a result of excitation of surface plasmon vibrations in the Fe nanoparticles.

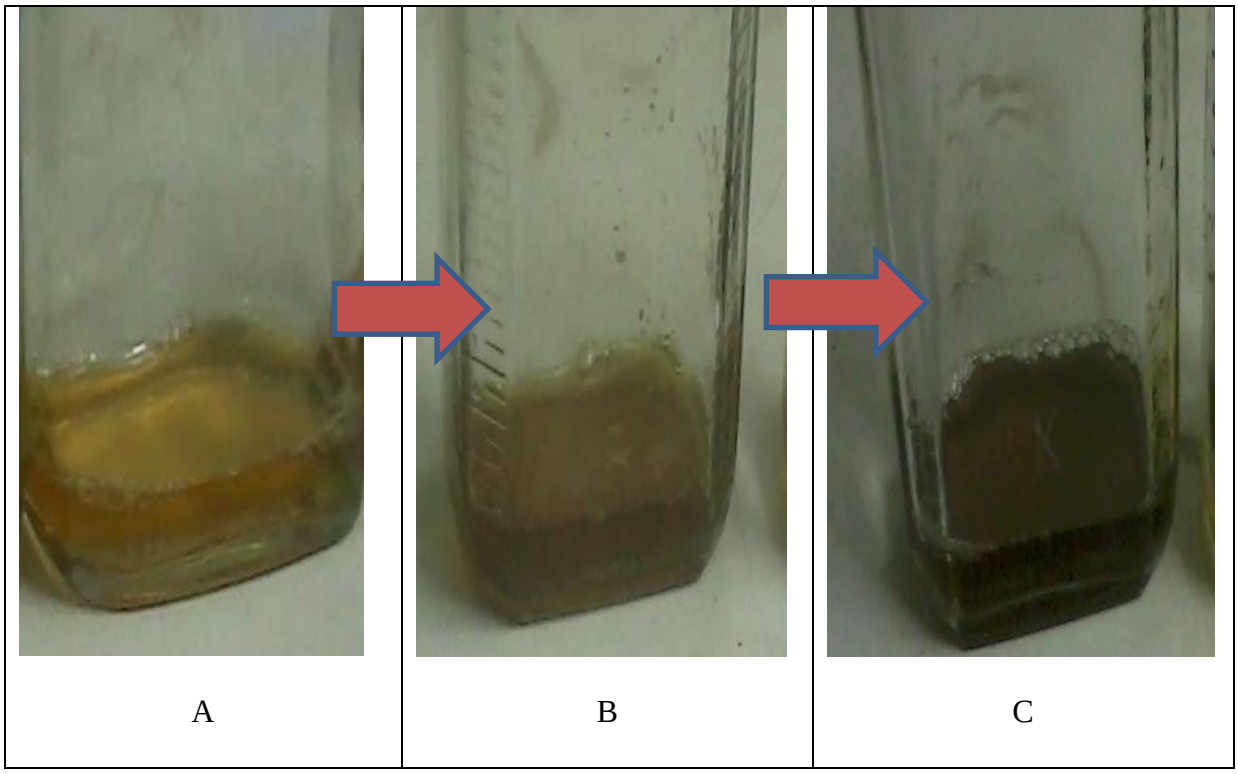

Figure 4.2: Visual inspection of the colour changes indicating formation of FeNPs; initially (A), after 2hours (B) and after 4hours (C).

4.2 UV-Vis analysis

The nanoparticles were first analysed using UV-Vis spectrophotometric techniques. The wavelength was scanned from 700 to 200nm giving the expected spectra (figure 4.3).

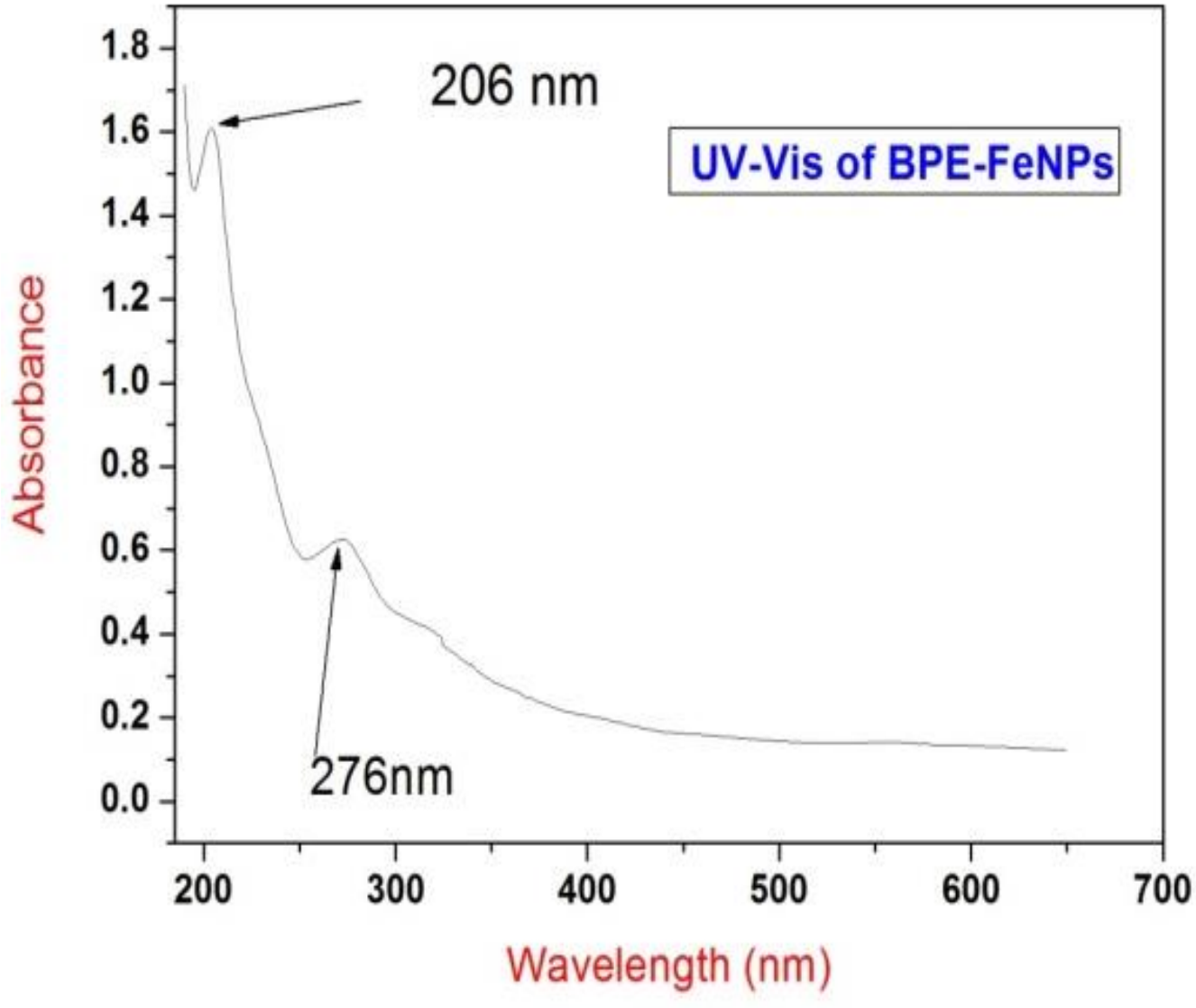

Figure 4.3: UV-Vis spectrum of BPE synthesised iron nanoparticles.

Iron nanoparticles formation was monitored visually and by the use of UV–Visible spectroscopy. Similar results on visual observations and a peak around 276 nm have been reported for eucalyptus leaf extract synthesized Fe nanoparticles (Wang *et al.*, 2014). Optimal conditions for the synthesis of iron nanoparticles in the present study were found to

be at pH 3.0, when 10 mg of the banana peels extracts were mixed with 1 mM of $FeCl_3$ at a temperature of 90 °C.

Table 4.1 shows calculation of the energy gap (Eg) of the Fe nanoparticles estimated using:

$$Eg = hc/\lambda$$

Where Eg is the energy gap (eV), h is Planck's constant, c is the velocity of light in m/s and λ is the wavelength where the absorbance value is maximum. The band gap energy is converted to eV because just like particles they require quantized energy to move through one volt.

Table 2: Calculation of the FeNPs band gap energy from the UV-Vis spectrum in Figure 4.2.

Band Gap Energy (E) = h*C/λ = 4.501eV				
h = Planks constant = 6.626 x 10^{-34} Joules sec				
C = Speed of light = 3.0 x 10^{8} meter/sec				
λ = Wavelength = 276 x 10^{-9}meters				
H	C	λ	E	eV
6.63E-34	3.00E+08	2.76E-07	0.0965E-17	4.501
Where 1eV = 1.6 X 10^{-19} Joules (conversion factor)				

4.3 TEM analysis

Transmission electron microscopy (TEM) method was utilised to investigate the synthesised nano-particles in order to determine their morphology and their size (Korgel *et al*.). Figure 4.4 demonstrate the results obtained.

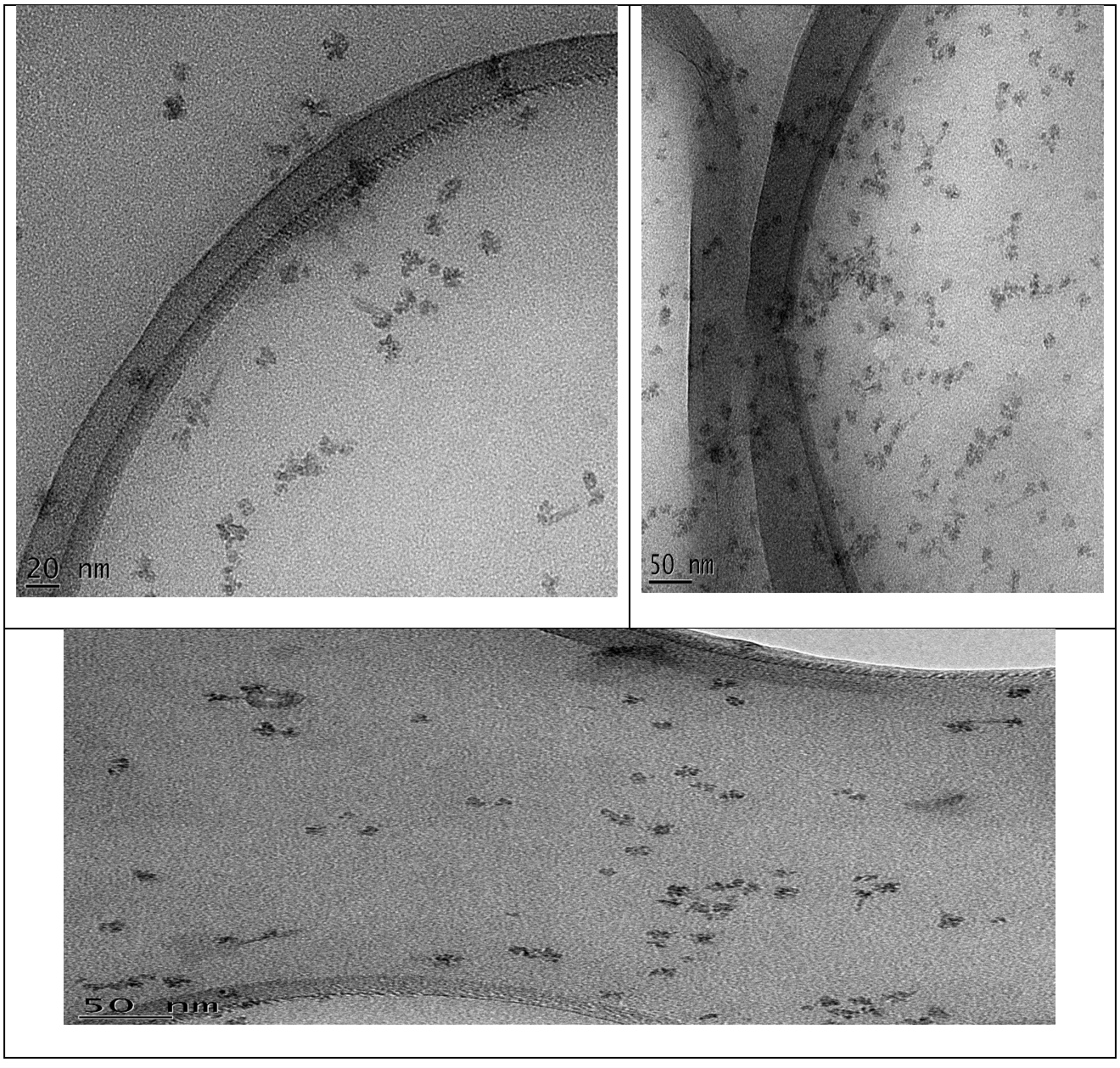

Figure 4.4: TEM images of the biosynthesised iron nanoparticles.

TEM images of biologically synthesized iron nanoparticles are shown in figure 4.4. From the TEM micrographs, the biologically synthesised nanoparticles are granular in nature and are dispersed throughout the grid.The particles are nanosized, with size ranging roughly between 20 nm and 50 nm.

Similar results of iron nanoparticles were obtained using different plant extracts (Vidya *et al*., 2013; Sheny *et al*., 2011; Shahwan *et al*., 2011; Singh *et al*.,2011; David *et al*., 2012).

4.4 EDS analysis

The EDS was exploited to reveal the elemental composition of the synthesized nanoparticles as is shown in (figure 4.5). These EDS values are useful in reflecting the nuclear content on the surface regions of the Fe nanoparticles.

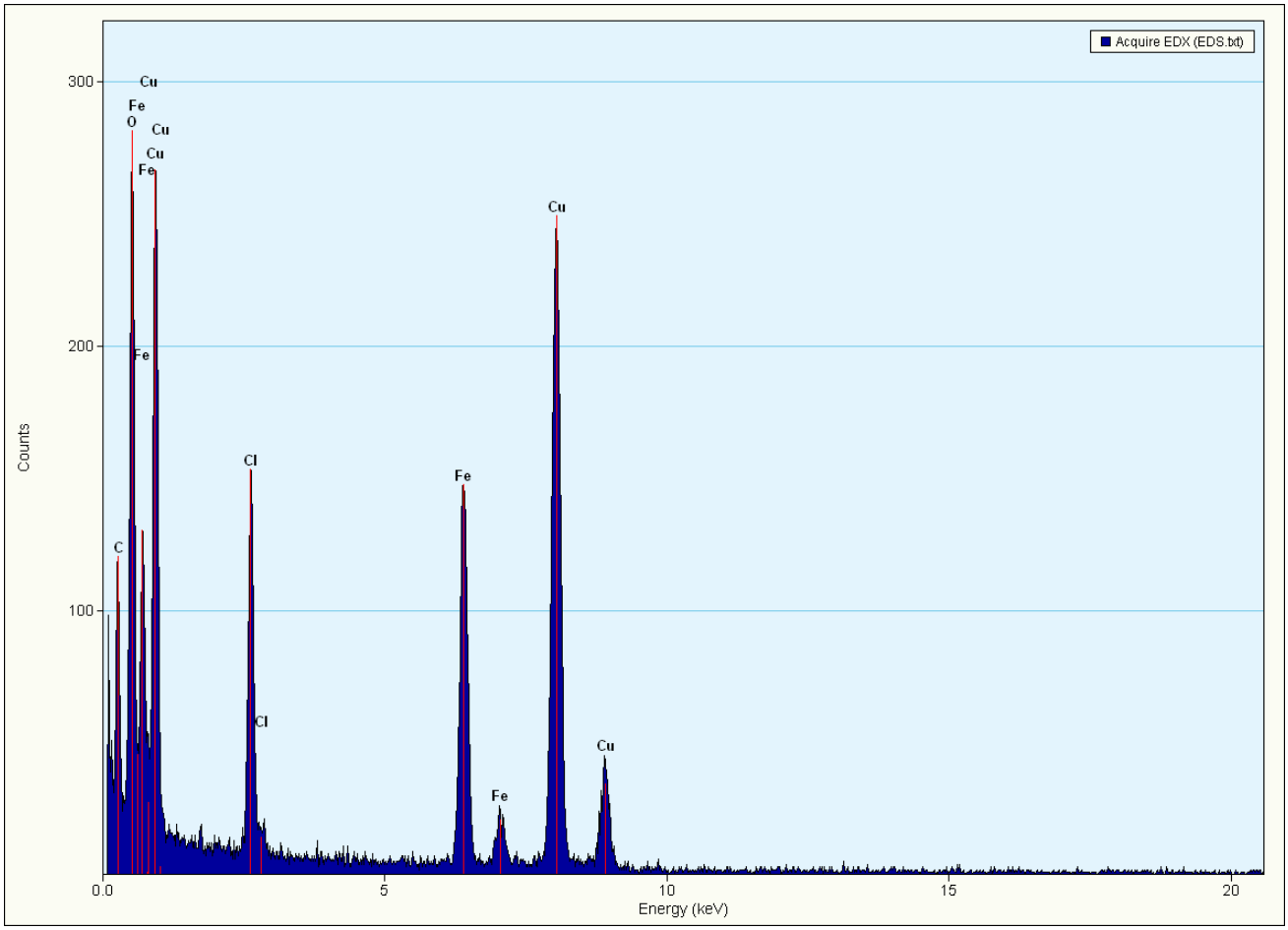

Figure 4.5: EDS spectrum of the biosynthesised iron nanoparticles.

The EDS profile showed intense peaks signals of iron at 182, 215, 424 and 458 energies. Other signals observed include that of chlorine, oxygen, carbon and copper. The oxygen and chlorine signals must be originating from $FeCl_3$ and BPE precursors respectively, utilised in the synthesis of BPE-FeNPs. The Carbon signals are credited mainly to the polyphenol groups and other Carbon containing molecules in the banana peels extracts. Copper signals were due to the copper grid onto which the sample was placed during the analysis. These results on the signature spectra are indicative of iron metal and are consistent with earlier reports (Hoag *et al*., 2009; Shahwan *et al*., 2011).

4.5 SEM analysis

The morphological studies and the structure of the synthesized Fe nanoparticles were analysed by scanning electron microscopy at a magnification of 2µm and 1µm as shown in figures 4.6 and 4.7.

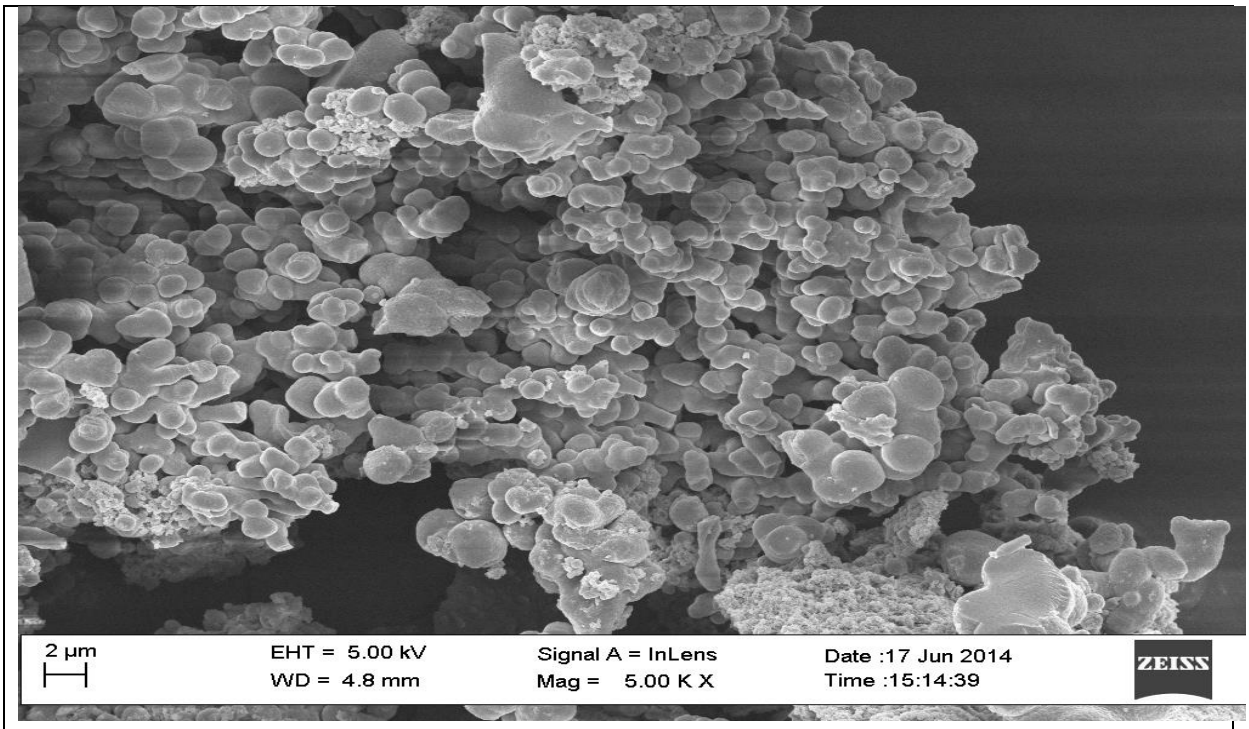

Figure 4.6: SEM images of the biosynthesised iron nanoparticles.

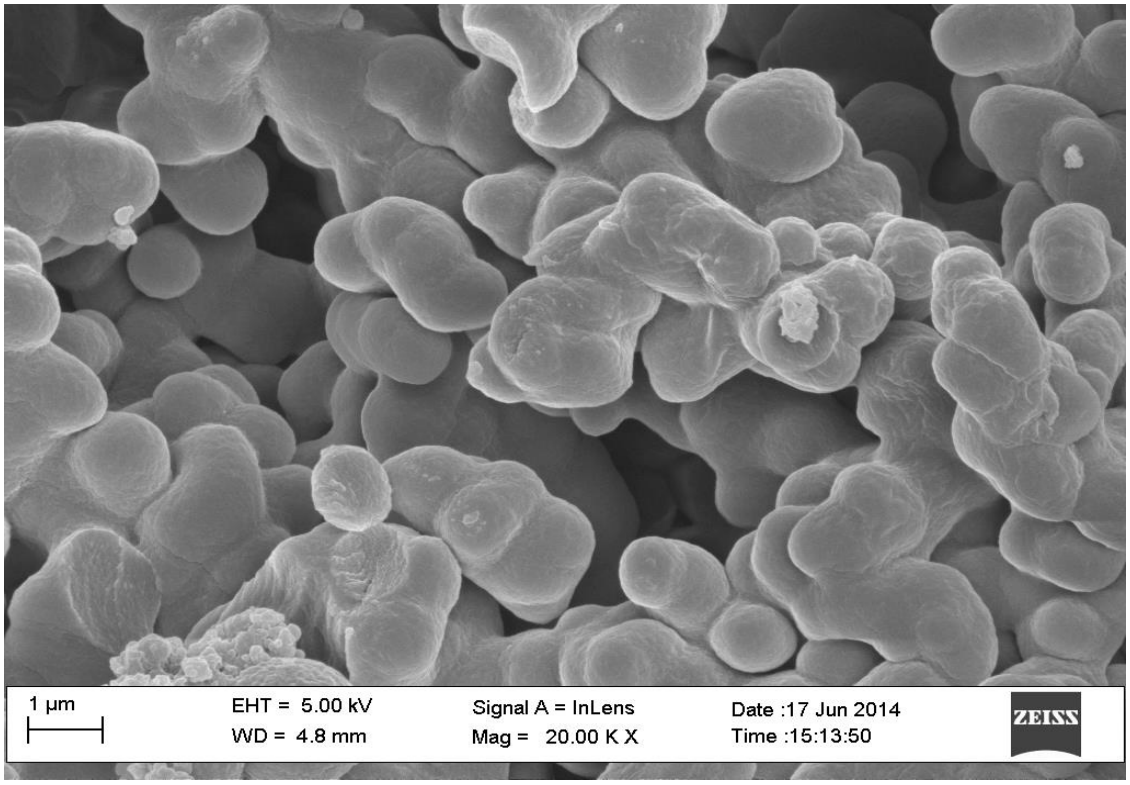

Figure 4.7: SEM images of the biosynthesised iron nanoparticles.

The SEM images of the iron nanoparticles obtained using reaction mixtures containing 10 mg of BPE powder and 1.0 mM of iron chloride, depicted that the shapes of the Fe nanoparticles were nearly round with smooth surfaces. All the nanoparticles were well separated with slight aggregation which agrees with TEM analyses. These SEM results were consistent with reported results of synthesized FeNPs using aqueous sorghum bran extracts as the reducing agent (Njagi *et al.,* 2010).

4.6 X-Ray diffractometer analysis (XRD)

The XRD analysis shown in figure 4.8 indicates that the synthesized Fe nanoparticles were amorphous with weak characteristic peak of iron, implying the non-crystalline nature of the iron nanoparticles.

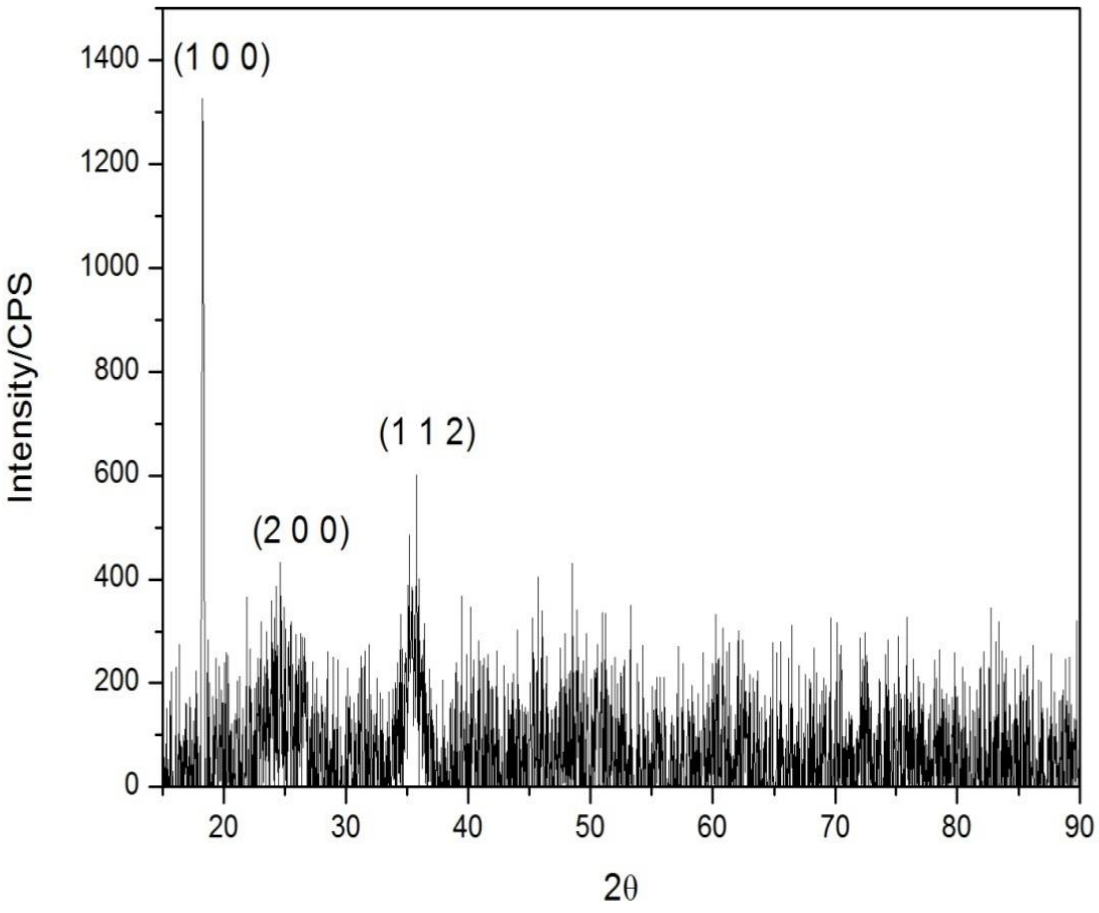

Figure 4.8: XRD spectra of biosynthesised iron nanoparticles.

The intense peaks observed at Bragg reflection 2θ=18.1466°, 24.6345° and 35.7775° were due to crystal planes of (110), (200) and (112) planes, respectively. These miller indices were used to confirm the presence of Fe nanoparticles.

The crystallite sizes were estimated using Scherrer's formula;

$D = K\lambda/\beta Cos\theta$

Where the D is the crystallite size, K is a constant taken to be 0.94, λ is the wavelength of X-ray, β is the half width of the most intense peak and θ is the Bragg angle of the most intense peak. Using this equation, the crystallite size was calculated to be 2.4383nm.

Table 3: Calculation of the synthesised iron nanoparticles diameter from the XRD spectra from (figure 4.8).

$D=K\lambda/\beta \cos\theta$
K=Dimensionless shape factor=0.94
λ =x-ray wavelength=1.54056 Å (CuKα radiation)
β= the full width at half maximum=0.5215^o
θ = position of the most intense peak=18.1466 ^{o}

K	λ	β	θ	D
0.9	1.54056	0.5215	18.08	2.4383nm

The unassigned peaks on the XRD pattern may show the crystallization of bio-natural phase present in the extract. This is indicative of some banana peels extracts adsorbed onto the formed iron nanoparticles since the extracts act as capping and stabilizing agents apparently protecting Fe from oxidation.

These results agree closely with the XRD results obtained for *Tridax procumbens* leaf extract which was used to synthesize pure Fe_3O_4 with a spinal structure (JCPDS, file PDF no.65-3107) (Senthil and Ramesh, 2012). Recent reports indicate that Fe nanoparticles produced by reduction with green tea (Nadagouda *et al*., 2010) and sorghum bran (Njagi *et al*,2010) extracts were also amorphous in nature. The three main peak positions and their respective indices are shown in table 4.8.

Table 4: Miller indices (h k l) and corresponding peak position obtained from the XRD pattern in figure 4.8.

h kl	Peak position
100	31.41
200	34.31
112	36.12

4.7 FTIR analysis

FTIR spectroscopy was used to show different functional groups on BPE and predict their role in iron nanoparticle synthesis (Figure 4.9).

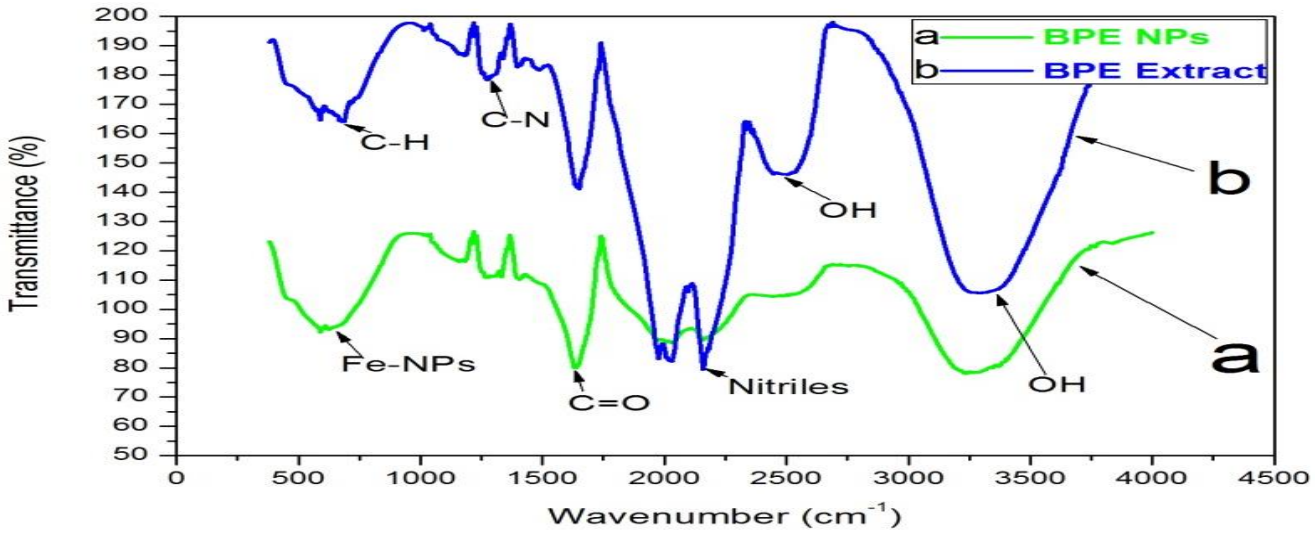

Figure 4.9: FTIR spectra of BPE iron nanoparticles (a) and BPE extract (b).

From the FTIR spectra, the O-H stretch at 3316 cm^{-1} was attributed to OH stretch in phenols present in the BPE. The peak located at around 2506cm^{-1} in the BPE was ascribed to the O–H stretching in carboxylic acids. The reduction in the peak intensity in the Fe nanoparticle spectra demonstrated that these groups maybe involved in the process of nanoparticle synthesis. The peak located at 1635 cm^{-1} could be assigned to the C=O stretch in carbonyls.

The nitriles stretch at 2133cm^{-1} in the BPE reduced in intensity and this shift showed the possible participation of nitrile groups of BPE concentrate in iron nanoparticles capping. The presence of C-H stretch of aromatics at 687cm^{-1} in the BPE spectrum and absence of the same peak in the nanoparticle spectrum indicated its involvement in the synthesis of the nanoparticles. A comparison of these results with earlier reports (Bankar *et al*., 2010) indicated that hydroxyl, carboxyl and amide groups in BPE might be participating in the process of nanoparticles synthesis.

The strong peak at 640cm^{-1}was attributed to nanoparticles vibrations and this further confirmed the synthesis of the nanoparticles.

4.8 Fabrication of the aptasensor

The cleaned GCE was treated by electrodeposition method of PANI followed by the FeNPs. The FeNPs/PANI/GCE fabricated electrode surface was then kept in a solution containing microcystin targeting aptamer to form an aptasensor that is Aptamer/FeNPs/PANI/GCE ready for detection of microcystin. A typical voltammogram of PANI being grown on an electrode through oxidative polymerization of 0.01 M aniline in 0.5 M HCl is shown in the subsequent figures 4.10 and 4.11. The potential was swept between –200mV and +1000 mV and back versus Ag/AgCl.

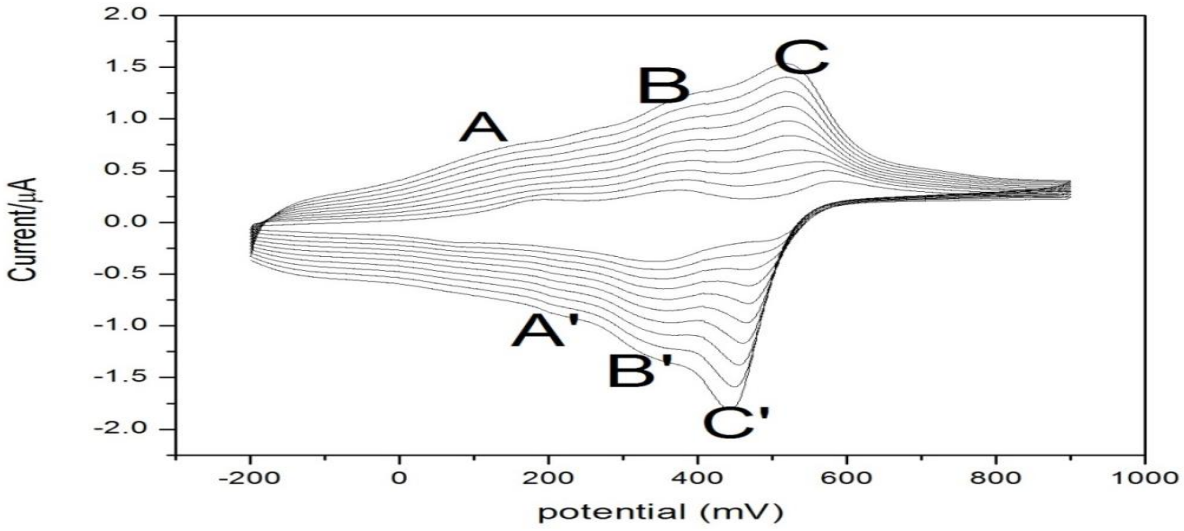

Figure 4.10: Electrodeposition of PANI onto the GCE at a scan rate of 50 mV/s.

Three peaks of reductive reaction and three peaks of oxidative reaction that were observed were consistent with the results obtained by Mathebe *et al*. (2004) and Iwuoha *et al*. (1997). The redox couple A /A' was ascribed to the conversion of PANI from reduced leucoemeraldine (LE) state to oxidized emeraldine (EM) state. The redox couple B/B' was as a result of redox reaction of p-benzoquinone and redox couple C/C' was ascribed to the transition from leucoemeraldine (LE) state to pernigraniline (PE) state followed by oxidation of the aniline monomer.

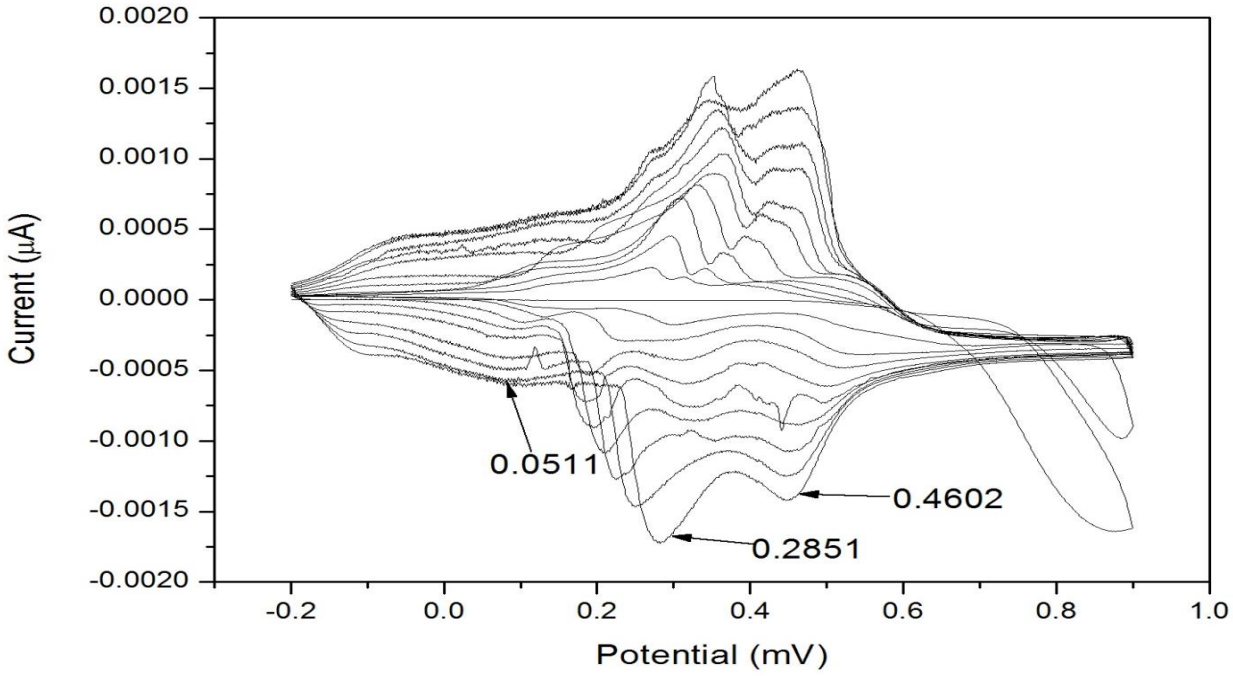

Figure 4.11: Electrodeposition of Fe nanoparticles onto PANI/GCE.

In the electrodeposition of the Fe nanoparticles onto the PANI/GCE, the voltammograms still had three sets of redox couples (A /A', B/B' and C/ C') though the peaks were not well defined. The three sets of redox couples were as a result of characteristic redox processes of PANI. The electron diffusion took place along the chain of the an adsorbed electroactive polymer (Kanungo *et al.,* 2002 and Bistolas *et al.*, 2005). The role of the PANI film in the aptasensor construction was thus to serve as a point of attachment for the nanoparticles and to boost the catalytic activity of aptamers for microcystin detection.

The peaks were well defined and remain unaltered during the cycles, reflecting the stability of the Fe nanoparticles coating onto the PANI/GCE and the strong interaction between PANI and Fe nanoparticles (Peulon and Lincot, 1998). The Aptasensor, Aptamer/ FeNPs/ PANI/ GCE was then used to detect the occurrence of microcystin in drinking water.

4.9 Sensing of the microcystin using the aptasensor

Sensing of Microcystin was based on the relative change in current response. Figure 4.12 shows electrochemical responses of the aptasensor before and after the addition of microcystin.

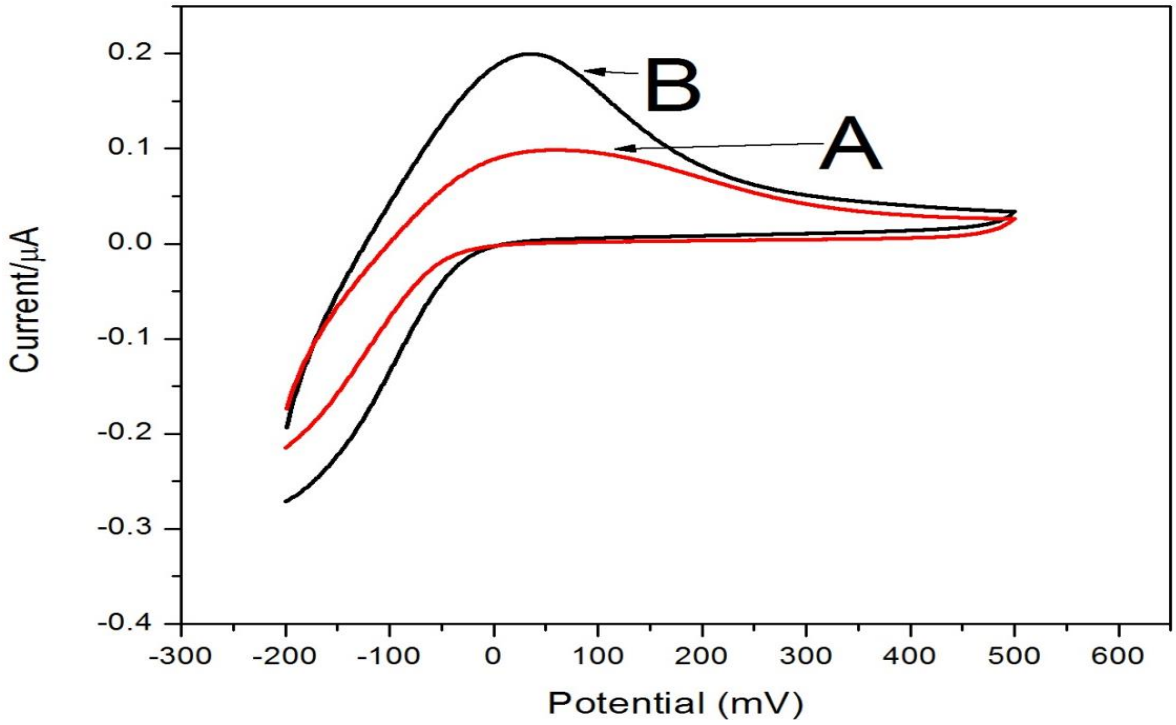

Figure 4.12: Electrochemical responses of the aptasensor before (B) and after (A) aggregation following addition of 0.1µM of microcystin at 37±1°C.

Figure 4.13 indicates the peak current when microcystin was introduced to Aptamer/FeNPs/PANI/GCE at different potential sweep. Where diagram A and B shows the half cycle voltammogram while C and D shows the full cyclic voltammogram before and after the addition of microcystin respectively.

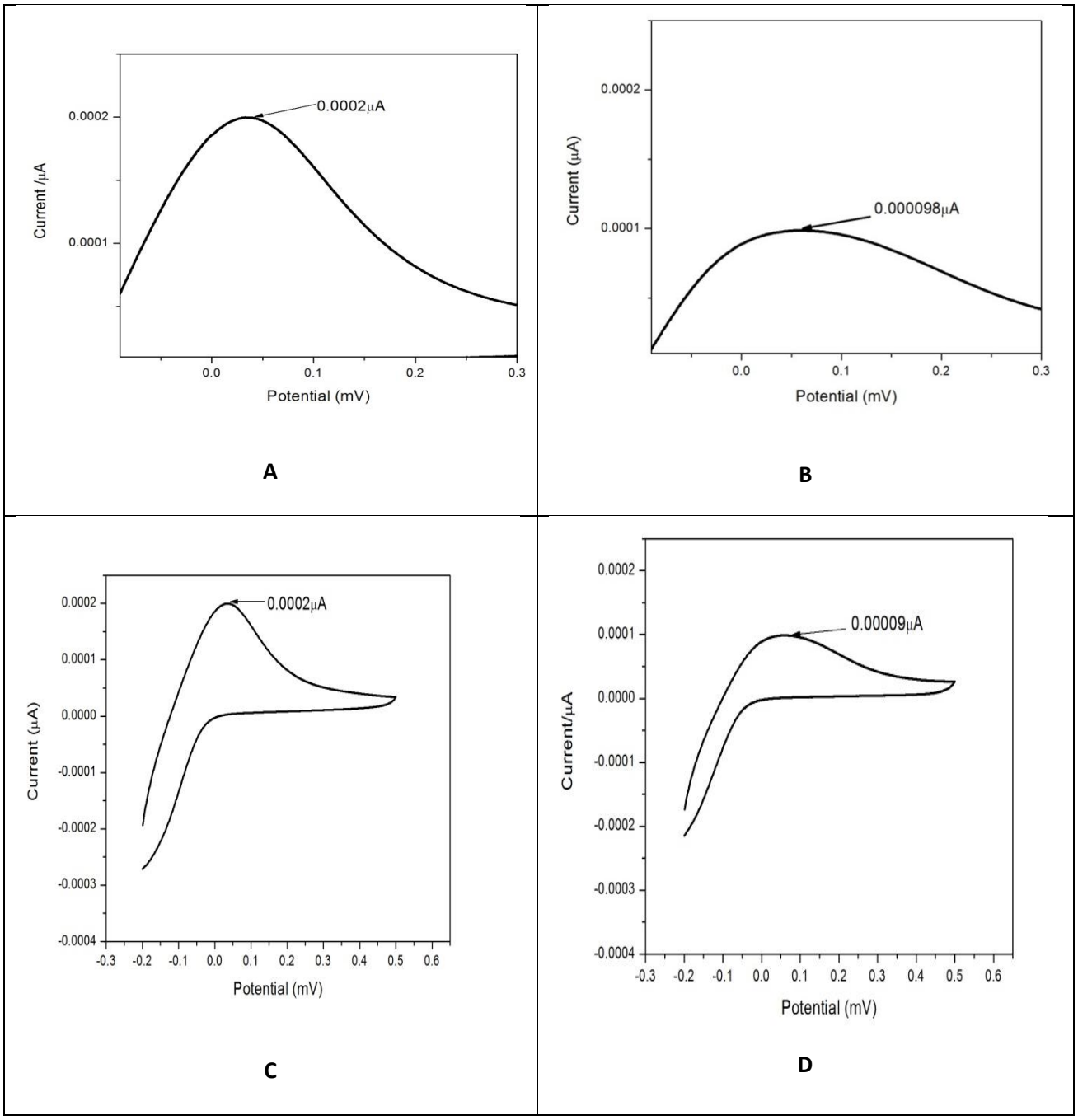

Figure 4.13: Peak Current of Microcystin/Aptamer/FeNPs/PANI/GCE.

The aggregation following the introduction of microcystin caused a sharp reduction in the peak current (Figure 4.13). This was as result of the binding of the microcystin to the aptamer, thereby decreasing the conductance of the aptamer immobilized on the Fe/PANI/GCE (Ellington, 1994).

4.10 Electroanalysis at different scan rates

Vital information can be obtained from the relationship between the peak current and different scan rates. Figure 4.14 shows cyclic voltammograms of the aptasensor electrochemical response towards microcystin at various scan rates. The effect of varying the scan rate (10-100mVs^{-1}) was investigated at constant concentration (0.5µM) of the microcystin.

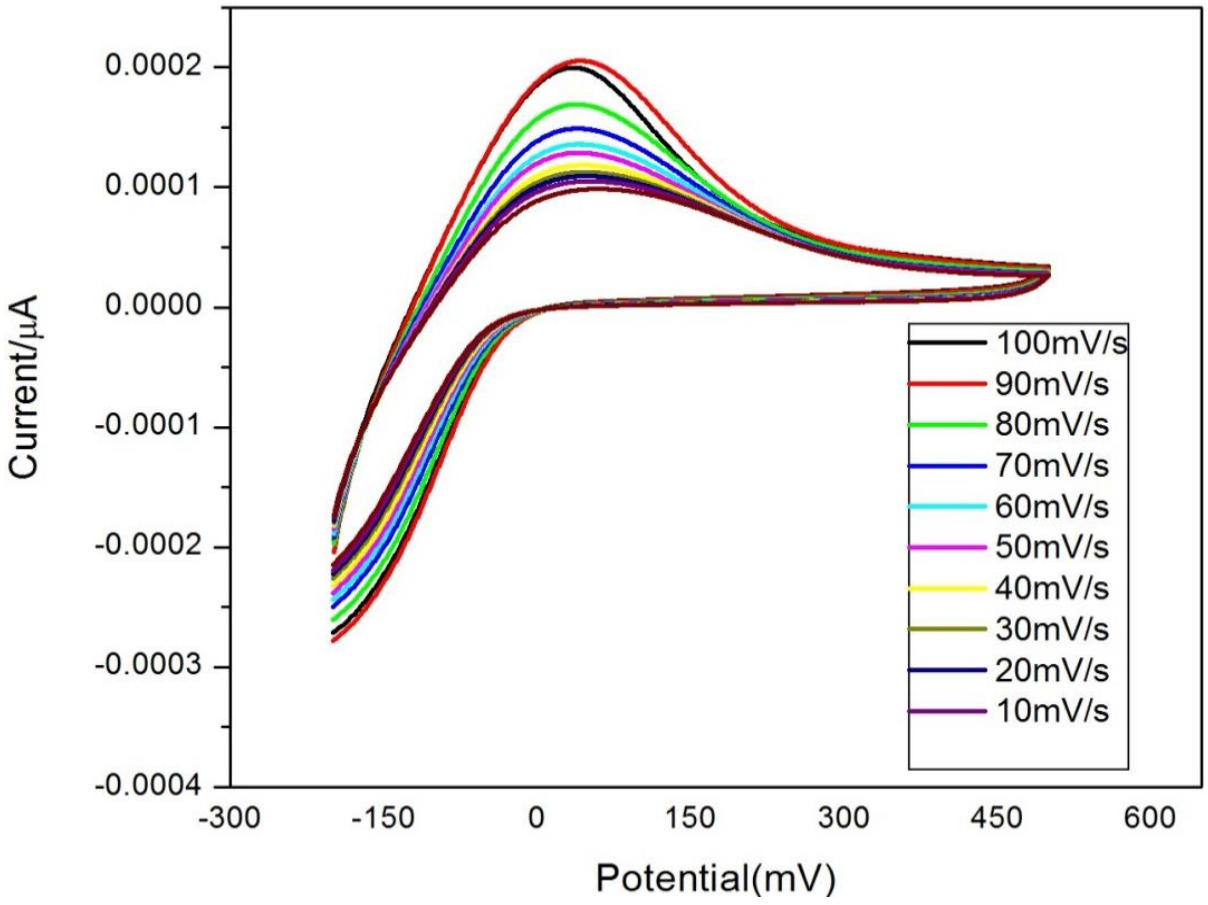

Figure 4.14: Cyclic voltammogram of aptasensor at different scan rates (10-100mV/s).

From figure 4.15 below, the anodic peak potential (36.0731mV) remained almost at the same position for all the scan rates and there was no corresponding reduction peak, indicating that the aptamer-microcystin oxidation event was indeed irreversible.

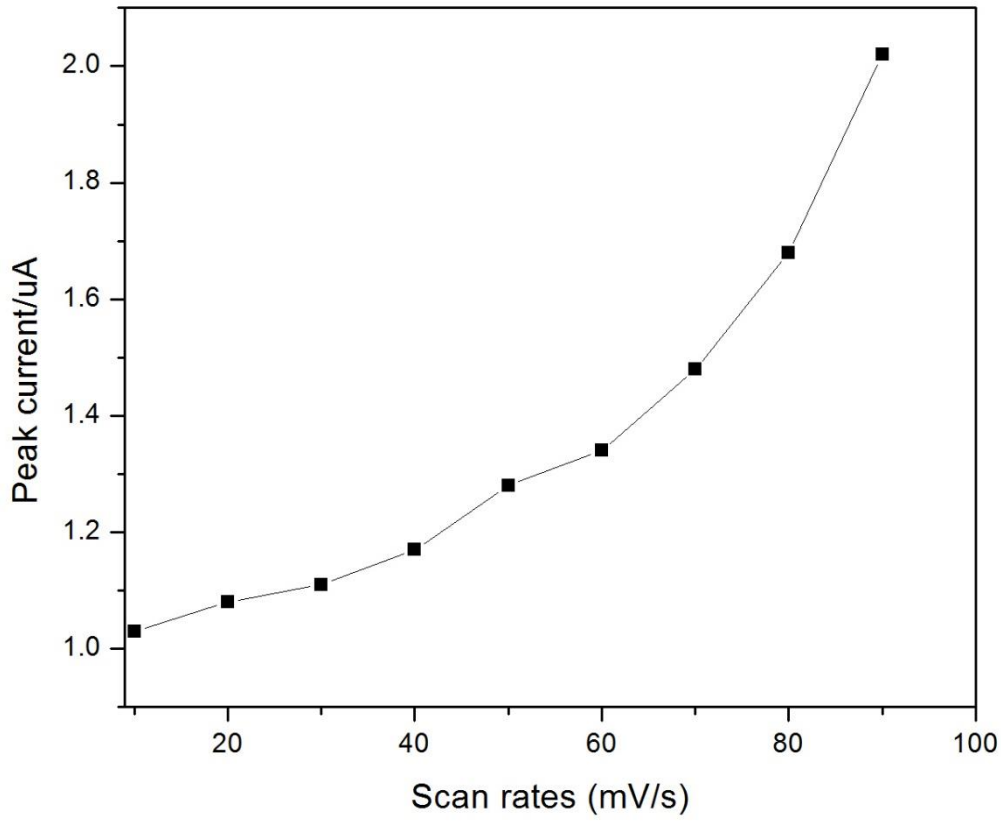

Figure 4.15: Peak current versus scan rate of MC-LR on PANI/FeNPs/GCE.

It is evident from figure 4.15 that current increased as the sweep rate increases in the range of 10 – 100 mV/s. This implies that the binding of the aptamer to MC-LR was an adsorption-controlled process that could be improved by pre-concentrating the MC-LR onto the surface of aptamer modified PANI/FeNPs/GCE.

4.11 Electroanalysis at different concentration

The aptasensor was applied as a biocompatible for determination of series of MC-LR concentrations (0.0 – 1.0μM). Cyclic voltammetry analyses were done to probe the coupling ability of the MC-LR using 1 μM aptamer immobilized on the surface of GCE/PANI/FeNPs (figure 4.16).

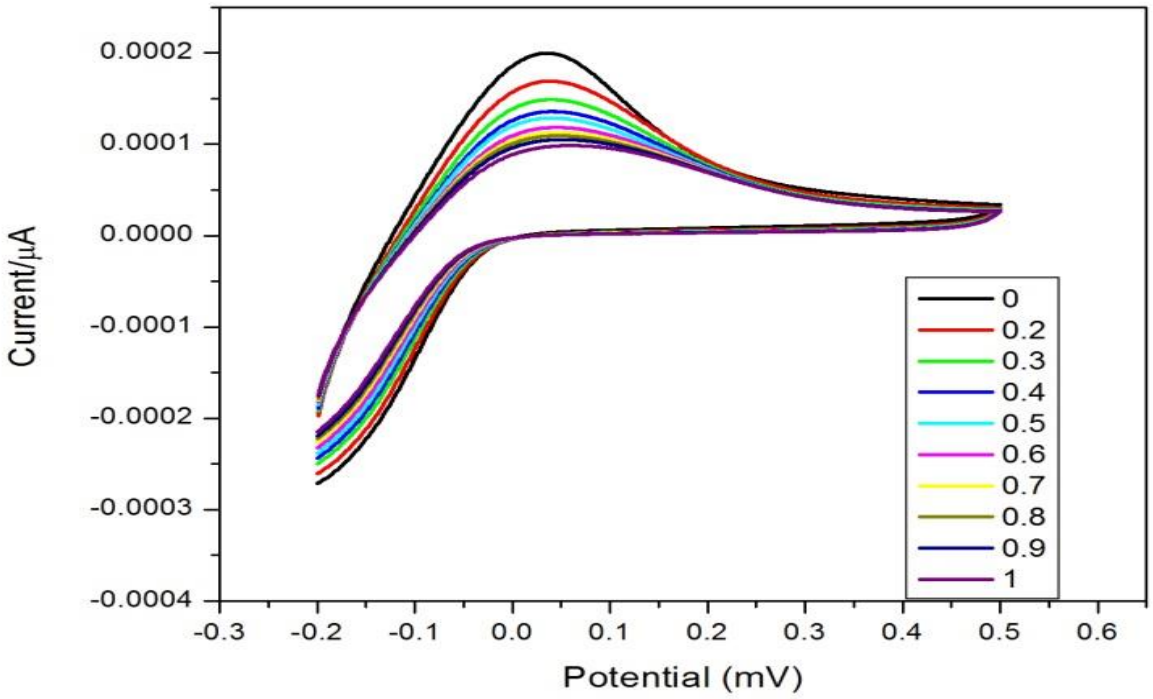

Figure 4.16: CV of aptasensor with different microcystin concentration (0-1μM) at a scan rate of 100 mV s^{-1}.

From figure 4.16 above, the peak current reduced with increased concentration of the microcystin. This was due to increase in the complex between aptamer and microcystin which cannot allow the transfer of electrons effectively.

The interaction of the aptamer with the MC-LR was confirmed by the drop in the peak current as the concentration of microcystin increases with a linear relationship, (R^2 = 0.97), as demonstrated in (figure 4.17). This decrease in peak current as MC-LR was being added was a consequence of the specific interaction of microcystin with the aptamer through an electrostatic repulsion that occurs between a negatively charged backbone of the aptamer and the negatively charged OH^- group of the microcystin.

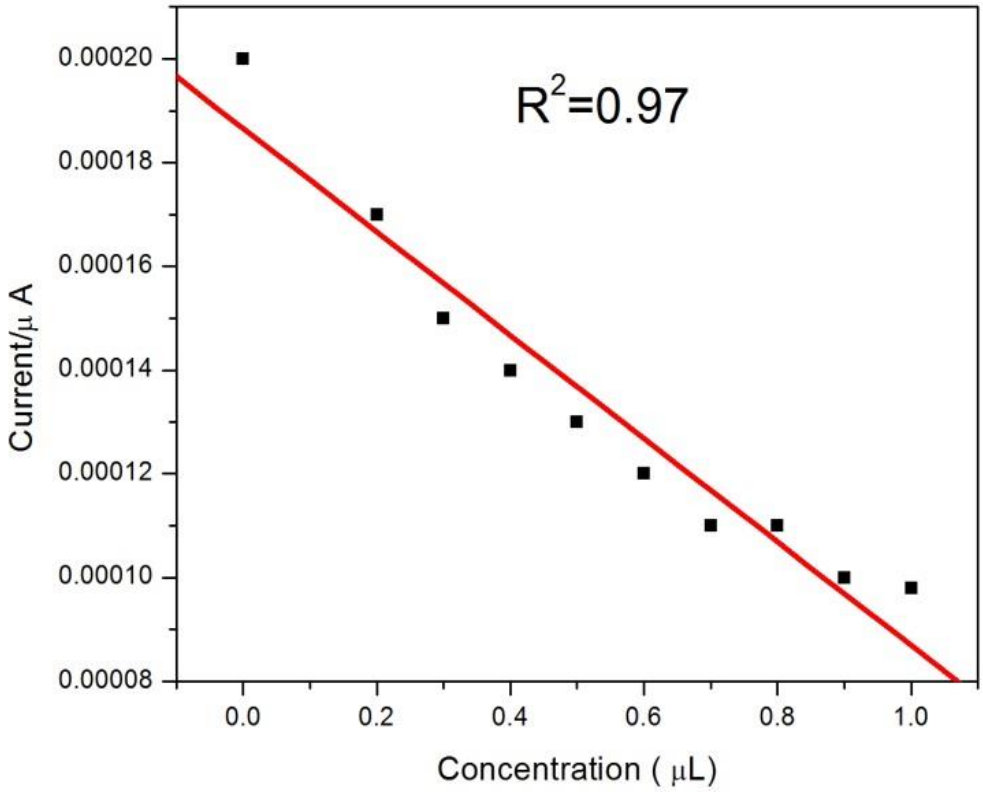

Figure 4.17: A calibration plot showing the relationship between peak current and concentration of microcystin.

The rate of diffusion of compound at the GCE / PANI/ FeNPs electrode is lowered by the formation of the MC-LR-aptamer complex that blocks the electron transfer to it (Kim *et al*., 2007). Fe nanoparticles provide a large specific surface area for increased immobilization of aptamer. The GCE/PANI/FeNPs nanocomposite provides effective adsorption centres that allow the active sites of the aptamer to be accessed easily.

After optimization of the dose response curve (figure 4.17) and based on the average standard deviation of the measurements (σ) and the slope (S) of the fitting curve as 3σ/S , the LOD for the aptasensor was determined at 0.06 µmol/litre.

The detection limit of this aptasensor was compared with that of DNA aptamer immobilized on gold terminal which was $0.3\mu ML^{-1}$ (Kim *et.al*., 2007) and the amperometric immunosensor using screen-printed electrodes which had a detection limit of $0.5\ \mu ML^{-1}$(Micheli *et.al*., 2005) as described earlier, under similar conditions and it was found that this aptasensor provided a better sensitivity. The detection limit of this aptasensor was also compared to the standard HPLC that reported a detection limit of $1.15\ \mu ML^{-1}$ (Mei et *al.*, 2007). Considering the range of microcystin concentrations (0.0−1.0µM) detectable in natural waters, the aptasensor developed in this work can be applied for detection of microcystin in natural or waste water samples.

CHAPTER FIVE

CONCLUSIONS

5.1 Conclusions

Iron nanoparticles were successfully synthesised using eco-friendly, rapid, simple and low cost approach through reduction of Iron chloride solution using banana peels extract. The usually discarded waste banana peels were therefore used effectively in this alternative method of synthesising iron nanoparticles.

Synthesised Fe nanoparticles were studied using visual observation, XRD, FTIR, TEM, UV-Vis and SEM techniques. The reaction mixture of ferric chloride and BPE displayed vivid colours confirming the synthesis of iron nanoparticles. UV–Vis spectra showing an absorption band at 206nm characteristic of the iron nanoparticles further affirmed the formation of the nanoparticles.

SEM images of the biosynthesized Fe nanoparticles at different magnifications showed that the particles were nearly round in shape with smooth surfaces. The TEM images revealed the nanoparticles were granular in nature with sizes in the range of 20-50 nm. EDS had strong iron signals at 182, 215, 424 and 458 energies confirming the synthesis of Fe nanoparticles.

X-ray diffraction investigations of the BPE synthesized Fe nanoparticles revealed that the nanoparticles were amorphous in nature with crystal planes at (110), (200) and (112) characteristic for iron nanoparticles. FTIR spectroscopy designated the contribution of banana peels extract's phenols, nitriles and carboxylic groups in the synthetic process.

These bio-inspired nanoparticles in turn were applied in devising a sensor for detecting Microcystins. The novel aptamer-based biosensing assay was developed for detection and quantification through observation of change in cyclic voltammogram upon microcystin

aptamer complex formation. The microcystin binding aptamer had a high binding affinity and specificity to its target and the electrochemical detection assay showed high reliability. The strong decrease in peak current observed in the cyclic voltammogram could be attributed to slowed charge transfer, brought about by the binding of MC-LR to aptamer. With the series of MC-LR dilutions tested it was found out that up to 0.06 μM L^{-1} was detectable with aptamer immobilized on the PANI/FeNPs nanocomposite platform. The high sensitivity of the aptasensor for the target was attributed to high surface area showed by the PANI/FeNPs nanocomposite, which essentially improved the aptamer loading.

5.2 Recommendations

1) Aptamer based sensors have shown ultra-high sensitivities for diagnosis and there is need to come up with real clinical samples for detecting Microcystins.
2) The aptasensor technique should be exploited and expanded to other diseases that are currently difficult to monitor.
3) Investigations should be done on the effect the nature of the supporting electrolyte (that is basic, acidic or neutral) may have on the microcystin sensing.
4) Study on the selectivity and specificity of the aptasensor should be done so as to eliminate interferences that may affect measurements.
5) The synthesis of Fe nanoparticles utilizing BPE should be done further to determine the mechanism of nanoparticle formation in order to adjust the procedure for large scale syntheses.
6) Nanoscience Laboratory should be established by the government of Kenya and University of Nairobi to facilitate further research on nanotechnology.

REFERENCES

Aki MA, Aly HF, Soliman HMA, Aref ME, Elrahman A, (2013) Preparation and Characterization of Silica Nanoparticles by Wet Mechanical Attrition of White and Yellow Sand. J. Nanomed. Nanotechnology . 4: 183.

Arnold, W. A., and Roberts, A. L. (2000). Pathways and kinetics of chlorinated ethylene and chlorinated acetylene reaction with Fe (0) particles. *Environmental Science & Technology*, **34**: 1794-1805.

Azevedo, S. M., Carmichael, W. W., Jochimsen, E. M., Rinehart, K. L., Lau, S., Shaw, G. R., & Eaglesham, G. K. (2002). Human intoxication by microcystins during renal dialysis treatment in Caruaru—Brazil. *Toxicology*, **181**, 441-446.

Bankar, A., Joshi, B., Kumar, A. R., and Zinjarde, S. (2010). Banana peel extract mediated novel route for the synthesis of silver nanoparticles. *Colloids and surfaces A: Physicochemical and engineering aspects*, **368**(1), 58-63.

Bard, A. J., and Faulkner, L. R. (1980). Electrochemical methods: fundamentals and applications (Vol. **2**). New York: Wiley.

Bell, R. (2012). *Introductory Fourier transform spectroscopy*. Elsevier.

Berezovski, M., Musheev, M., Drabovich, A., and Krylov, S. N. (2006). Non-SELEX selection of aptamers. *Journal of the American Chemical Society*, *128*(**5**), 1410-1411.

Best, R., Lewis, D. A., & Nasser, N. (1984). The anti-ulcerogenic activity of the unripe plantain banana (Musa species). *British journal of pharmacology*, **82**: 107-116.

Bhattacharya, R., and Mukherjee, P. (2008). Biological properties of "naked" metal nanoparticles. *Advanced drug delivery reviews*, **60**: 1289-1306.

Bistolas, N., Wollenberger, U., Jung, C., and Scheller, F. W. (2005) Cytochrome P450 biosensors—a review *Biosensors and Bioelectronics*, **20**: 2408-2423.

Bose, S., Kuila, T., Uddin, M. E., Kim, N. H., Lau, A. K., & Lee, J. H. (2010). In-situ synthesis and characterization of electrically conductive Polypyrrole/graphene nanocomposites. *Polymer*, **51**: 5921-5928.

Cai, H., Lee, T. M. H., & Hsing, I. M. (2006). Label-free protein recognition using an aptamer-based sensor.

Chou, Y. H., Lin, Y. S., Wu, S. H., Hung, Y., Chang, C., Lin, M. L., ... & Mou, C. Y. (2006). Multifunctional composite nanoparticles: magnetic, luminescent, and mesoporous. *Chemistry of Materials*, **18**: 5170-5172.

Cullity, B.D. (1978) Elements of X-ray Diffraction, 2nd ed., Addison-Wesley, Menlo Park, CA, pp. 101–102.

De Souza, S. (2007). Smart coating based on polyaniline acrylic blend for corrosion protection of different metals. *Surface and Coatings Technology*, **201**(16), 7574-7581.

Deng, Q., Watson, C. J., and Kennedy, R. T. (2003). Aptamer affinity chromatography for rapid assay of adenosine in microdialysis samples collected in vivo. *Journal of Chromatography A*, **1005**: 123-130.

Dubey, S. P., Lahtinen, M., and Sillanpää, M. (2010) Green synthesis and characterizations of silver and gold nanoparticles using leaf extract of Rosa rugosa *Colloids and Surfaces A: Physicochemical and Engineering Aspects*, **364**: 34-41.

Duke P. J., (1990) Modern Microscopies: Techniques and Applications, Plenum Press, New York.

Durán, N., Marcato, P. D., Durán, M., Yadav, A., Gade, A., & Rai, M. (2011). Mechanistic aspects in the biogenic synthesis of extracellular metal nanoparticles by peptides, bacteria, fungi and plants. *Applied microbiology and biotechnology*, **90**: 1609-1624.

Eissa, S., Ng, A., Siaj, M., & Zourob, M. (2014). Label-free voltammetric aptasensor for the sensitive detection of microcystin-LR using graphene-modified electrodes. *Analytical chemistry*, **86(**15), 7551-7557.

Ellington, A. D. (1994). RNA selection: Aptamers achieve the desired recognition. *Current Biology*, **4**(5), 427-429.

Elliott. D.W. and Zhang, W. X. (2006). Applications of iron nanoparticles for groundwater remediation; *Remediation Journal*. **16** (2): 7-21.

Fang, X., and Tan, W. (2009). Aptamers generated from cell-SELEX for molecular medicine: a chemical biology approach. *Accounts of chemical research*, *43* (**1**), 48-57.

Fodey, T., Leonard, P., O'Mahony, J., O'Kennedy, R., and Danaher, M. (2011). Developments in the production of biological and synthetic binders for immunoassay and sensor-based detection of small molecules. *TrAC Trends in Analytical Chemistry*, **30** (2), 254-269.

Griffiths, P. R. (1975). *Chemical infrared Fourier transform spectroscopy*. Wiley.

Gopinath, S. C. B. (2007). Methods developed for SELEX. *Analytical and bioanalytical chemistry*, *387* (**1**), 171-182.

Gupta, A. K., & Wells, S. (2004). Surface-modified superparamagnetic nanoparticles for drug delivery: preparation, characterization, and cytotoxicity studies. *NanoBioscience, IEEE Transactions on*, **3** (1), 66-73.

Hadjipanayis, G. C., & Siegel, R. W. (Eds.). (2012). *Nanophase materials: Synthesis-properties-applications* (Vol. **260**). Springer Science & Business Media.

Herr, J. K., Smith, J. E., Medley, C. D., Shangguan, D., and Tan, W. (2006) Aptamer-conjugated nanoparticles for selective collection and detection of cancer cells. *Analytical Chemistry*, **78**: 2918-2924.

Hoag, G. E., Collins, J. B., Holcomb, J. L., Hoag, J. R., Nadagouda, M. N., & Varma, R. S. (2009). Degradation of bromothymol blue by 'greener'nano-scale zero-valent iron synthesized using tea polyphenols. *Journal of Materials Chemistry*, **19** (45), 8671-8677.

Horiuchi, S. and Nakao, Y. (2007) Polymer/metal nanocomposites: Assembly of metal nanoparticles in polymer films and their applications. *Curr Nanosci*, **3**: 206-214..

Huang, G. Y., Ma, L. F., Guan, M. Y., Liang, J. T., Huang, Y., & Li, G. Y. (2015, July). A Novel hig E Aptamer Biosensor Base on Core-Shell Fe_3O_4 Au Magnetic Composite Nanoparticles. In *Advanced Materials Research* (Vol. **1118**, pp. 170-175). Trans Tech Publications.

Huber, D. L. (2005). Synthesis, properties, and applications of iron nanoparticles. *Small*, **5**, 482-501.

Ibelings, B. W., Bruning, K., De Jonge, J., Wolfstein, K., Pires, L. D., Postma, J., & Burger, T. (2005). Distribution of microcystins in a lake foodweb: no evidence for biomagnification. *Microbial Ecology*, **49** (4), 487-500.

Iwuoha, E. I., Saenz de Villaverde, D., Garcia, N. P., Smyth, M. R., and Pingarron, J. M. (1997) Reactivities of organic phase biosensors. 2. The amperometric behaviour of horseradish peroxidase immobilised on a platinum electrode modified with an electrosynthetic polyaniline film. *Biosensors and Bioelectronics*, **12**: 749-761.

Jeong, S. I., Kim, B. S., Kang, S. W., Kwon, J. H., & Lee, Y. M. (2004). POLYMER CONTENTS 731© 2004 Elsevier. *Biomaterials*, *25*, 28.

Kanungo, M., Kumar, A., and Contractor, A. Q. (2002) Studies on electropolymerization of aniline in the presence of sodium dodecyl sulfate and its application in sensing urea. *Journal of Electroanalytical Chemistry*, **528***:*46-56.

Karlsson, H. L., Cronholm, P., Gustafsson, J., & Moller, L. (2005). Copper oxide nanoparticles are highly toxic: a comparison between metal oxide nanoparticles and carbon nanotubes. *Chemical research in toxicology*, **21:**1726-1732.

Kellner, C., Botero, M. L., Latta, D., Drese, K., Fragoso, A., and O'Sullivan, C. K. (2011). Automated microsystem for electrochemical detection of cancer markers. *Electrophoresis*, **32** (8), 926-930.

Khreich, N., Lamourette, P., Renard, P. Y., Clavé, G., Fenaille, F., Créminon, C., & Volland, H. (2009). A highly sensitive competitive enzyme immunoassay of broad specificity quantifying microcystins and nodularins in water samples. *Toxicon*, **53** (5), 551-559.

Kim, Y. S.; Jung, H. S.; Matsura, T.; Lee, H. Y.; Kawai, T.; Gu, M. B. (2007) Electrochemical detection of 17β-estradiol using a DNA aptamer immobilized gold electrode chip. Biosens. Bioelectron., **22**, 2525−2531.

Korgel, B. A., Fullam, S., Connolly, S., and Fitzmaurice, D. (1998). Assembly and self-organization of silver nanocrystal superlattices: ordered "soft spheres". *The Journal of Physical Chemistry B*, **102** (43), 8379-8388.

Kumar, C.S.S.R. 2006. Nanomaterials: Toxicity, Health and Environmental Issues. Wiley-VCH, Germany.

Kuhn, A.,Garrigue, P., Delville, M. H., Labrugère, C., Cloutet, E., Kulesza, P. J., and Morand, J. P. (2004). Top-down approach for the preparation of colloidal carbon nanoparticles. *Chemistry of materials*, **16** (16), 2984-2986.

Kumar, K. S., Sajwan, K. S., Richardson, J. P., & Kannan, K. (2008). Contamination profiles of heavy metals, organochlorine pesticides, polycyclic aromatic hydrocarbons and alkylphenols in sediment and oyster collected from marsh/estuarine Savannah GA, USA. *Marine Pollution Bulletin*, **56** (1), 136-149.

Lahti, K., Rapala, J., Färdig, M., Niemelä, M., & Sivonen, K. (1997). Persistence of cyanobacterial hepatotoxin, microcystin-LR in particulate material and dissolved in lake water. *Water Research*, **31** (5), 1005-1012.

Lin, Y. S., Wu, S. H., Hung, Y., Chou, Y. H., Chang, C., Lin, M. L., ... & Mou, C. Y. (2006). Multifunctional composite nanoparticles: magnetic, luminescent, and mesoporous. *Chemistry of Materials*, *18* (22), 5170-5172.

Lindner, P., Molz, R., Yacoub-George, E., Dürkop, A., and Wolf, H. (2004). Development of a highly sensitive inhibition immunoassay for microcystin-LR. *Analytica chimica acta*, **521** (1), 37-44.

Liu, G., Lin, Y. Y., Wang, J., Wu, H., Wai, C. M., and Lin, Y. (2007) Disposable electrochemical immunosensor diagnosis device based on nanoparticle probe and immunochromatographic strip. *Analytical chemistry*, **79** (20), 7644-7653.

Lo, I.M.-C., R.Y. Surampalli, and K.C.K. Lai (2009) Zero-Valent Iron Reactive Materials for Hazardous Waste and Inorganic Removal. ASCE Publications, Reston, VA.

Long, F., He, M., Zhu, A. N., & Shi, H. C. (2009). Portable optical immunosensor for highly sensitive detection of microcystin-LR in water samples. *Biosensors and Bioelectronics*, **24** (8), 2346-2351.

Mascini, M., Tombelli, S., and Minunni, M., (2007) Aptamers-based assays for diagnostics, environmental and food analysis. *Biomolecular engineering*, **24** (2), 191-200.

Mathebe, N. G., Morrin, A., and Iwuoha, E. I. (2004) Electrochemistry and scanning electron microscopy of polyaniline/peroxidase-based biosensor. *Talanta*, **64**: 115-120.

Mei, Z., Chu, H., Chen, W., Xue, F., Liu, J., Xu, H., & Zheng, L. (2013). Ultrasensitive one-step rapid visual detection of bisphenol A in water samples by label-free aptasensor. *Biosensors and Bioelectronics*, *39* (1), 26-30.

Messineo, V., Bogialli, S., Melchiorre, S., Sechi, N., Lugliè, A., Casiddu, P., and Bruno, M. (2009). Cyanobacterial toxins in Italian freshwaters. *Limnologica-Ecology and Management of Inland Waters*, **39** (2), 95-106.

Micheli, L., Grecco, R., Badea, M., Moscone, D., & Palleschi, G. (2005). An electrochemical immunosensor for aflatoxin M1 determination in milk using screen-printed electrodes. *Biosensors and Bioelectronics*, *21* (4), 588-596.

Mokbel, M. S., & Hashinaga, F. (2005). Antibacterial and antioxidant activities of banana (Musa, AAA cv. Cavendish) fruits peel. *Am J Biochem Biotechnol*, *1* (**3**), 125-131.

Moreira, C., Ramos, V., Azevedo, J., & Vasconcelos, V. (2014). Methods to detect cyanobacteria and their toxins in the environment. *Applied microbiology and biotechnology*, **98** (19), 8073-8082.

Mountfort, D. O., Holland, P., & Sprosen, J. (2005). Method for detecting classes of microcystins by combination of protein phosphatase inhibition assay and ELISA: comparison with LC-MS. *Toxicon*, **45**:199-206.

Nadagouda, M. N., Castle, A. B., Murdock, R. C., Hussain, S. M., & Varma, R. S. (2010). In vitro biocompatibility of nanoscale zerovalent iron particles (NZVI) synthesized using tea polyphenols. *Green Chemistry*, **12** (1), 114-122.

Nagata, S., Tsutsumi, T., Hasegawa, A., Yoshida, F., Ueno, Y., and Watanabe, M. F. (1997) Enzyme immunoassay for direct determination of microcystins in environmental water. *Journal of AOAC International*, **80**: 408-417.

Narayanan, K. B., & Sakthivel, N. (2010). Biological synthesis of metal nanoparticles by microbes. *Advances in colloid and interface science*, **156**: 1-13.

Niazi, J. H., Lee, S. J., Kim, Y. S., and Gu, M. B. (2008). ssDNA aptamers that selectively bind oxytetracycline. *Bioorganic & medicinal chemistry*, **16**:1254-1261.

Njagi, E. C., Huang, H., Stafford, L., Genuino, H., Galindo, H. M., Collins, J. B and Suib, S. L. (2011). Biosynthesis of iron and silver nanoparticles at room temperature using aqueous sorghum bran extracts. *Langmuir*, **27** (1), 264-271.

Nuxoll, E.E., T. Shimotori, W.A. Arnold, E.L. Cussler. (2003). Iron Nanoparticles in Reactive Environmental Barriers. Presentation at the AIChE Annual Meeting, November 20, 2003.

Ortelli, D., Edder, P., Cognard, E., and Jan, P. (2008). Fast screening and quantitation of microcystins in microalgae dietary supplement products and water by liquid chromatography coupled to time of flight mass spectrometry. *Analytica chimica acta*, **617** (1), 230-237.

Pattanayak, M., and Nayak, P. L. (2013). Ecofriendly green synthesis of iron nanoparticles from various plants and spices extract. *International Journal of Plant, Animal and Environmental Sciences*, **3**, 68-78.

Peulon, S., and Lincot, D. (1998). Mechanistic study of cathodic electrodeposition of zinc oxide and zinc hydroxychloride films from oxygenated aqueous zinc chloride solutions. *Journal of the Electrochemical Society*, **145** (3), 864-874.

Pyo, D., Choi, J., Hong, J., & Hlaing Oo, H. (2006). Rapid analytical detection of microcystins using gold colloidal immunochromatographic strip. *Journal of Immunoassay and Immunochemistry*, **27** (4), 291-302.

Rabolt, J. F., Burns, F. C., Schlotter, N. E., & Swalen, J. D. (1983). Anisotropic orientation in molecular monolayers by infrared spectroscopy. *The Journal of Chemical Physics*, **78** (2), 946-952.

Ricci, D., Olivieri, F., Buzzi, F., Carena, E., Fumagalli, R., Maierna, M., and Volante, M. (2007, May) Contamination of some lakes from cyanobacteria toxins and related oligo-peptides in lombardy: a real case. In *Simposio Internazionale: le Tossine Algali, Università di Trieste-SITOX, Trieste* (pp. 27-29).

Riley, P. J., and Wallace, G. G. (1991). Intelligent chemical systems based on conductive electroactive polymers. *Journal of intelligent material systems and structures*, **2** (2), 228-238.

Sangolkar, L. N., Maske, S. S., & Chakrabarti, T. (2006). Methods for determining microcystins (peptide hepatotoxins) and microcystin-producing cyanobacteria. *Water research*, **40** (19), 3485-3496.

Savage, D., Wilson, J., Cressey, G., Cressey, B., Cuadros, J., Ragnarsdottir, K. V., & Shibata, M. (2006). The effect of iron on montmorillonite stability (II) Experimental investigation. *Geochimica et Cosmochimica Acta*, **70**, 323-336.

Senthil, M., and Ramesh, C. (2012) Biogenic synthesis of Fe 3 o 4 nanoparticles using *Tridax procumbens* leaf extract and its antibacterial activity on *Pseudomonas aeruginosa*. *Digest Journal of Nanomaterials & Biostructures (DJNB)*, **7** (4).

Senzaki, T. and Y. Kumagai. (1988) Treatment of 1, 1, 2, 2-Tetrachloroethane with iron powder. *Kogyo Yosui*. **357** (1): 2-7.

Shahwan, T., Sirriah, S. A., Nairat, M., Boyaci, E., Eroğlu, A. E., Scott, T. B., and Hallam, K. R. (2011). Green synthesis of iron nanoparticles and their application as a Fenton-like catalyst for the degradation of aqueous cationic and anionic dyes. *Chemical Engineering Journal*, **172** (1), 258-266.

Sheny D., Mathew J., and Philip D. (2011) "Phytosynthesis of Au, Ag and Au-Ag bimetallic nanoparticles using aqueous extract and dried leaf of *Anacardium occidentale*. *Spectrochimica Acta Part A* **79:** 254–262.

Singh, R., Shukla, V., Yadav, R., Sharma, P., Singh, P., and Pandey, A. (2011); Biological approach of zinc oxide nanoparticles formation and its characterization. *Mat Lett*. **2:** 313–317.

So, H. M., Won, K., Kim, Y. H., Kim, B. K., Ryu, B. H., Na, P. S., and Lee, J. O. (2005). Single-walled carbon nanotube biosensors using aptamers as molecular recognition elements. *Journal of the American Chemical Society*, **127**: 11906-11907.

Someya, S., Yoshiki, Y., & Okubo, K. (2002). Antioxidant compounds from bananas (Musa Cavendish). *Food Chemistry*, **79**: 351-354.

Song, S., Wang, L., Li, J., Fan, C., & Zhao, J. (2008). Aptamer-based biosensors. *TrAC Trends in Analytical Chemistry*, **27**:108-117.

Speets, E. A., Dordi, B., Ravoo, B. J., Oncel, N., Hallbäck, A. S., Zandvliet, H. J., & Reinhoudt, D. N. (2005). Noble Metal Nanoparticles Deposited on Self Assembled Monolayers by Pulsed Laser Deposition Show Coulomb Blockade at Room Temperature. *Small, 1* (**4**), 395-398.

Spinks, G. M., Dominis, A. J., Wallace, G. G., & Tallman, D. E. (2002). Electroactive conducting polymers for corrosion control. *Journal of Solid State Electrochemistry***, 6** (2), 85-100.

Stoltenburg, R., Reinemann, C., & Strehlitz, B. (2007). SELEX—a (r) evolutionary method to generate high-affinity nucleic acid ligands. *Biomolecular engineering*, *24* (**4**), 381-403.

Treacy, M. M., & Higgins, J. B. (2007). Collection of Simulated XRD Powder Patterns for Zeolites *5th Revised Edition*. Elsevier.

Uslu, B., and Özkan, S. A. (2002). Electrochemical characterisation of nefazodone hydrochloride and voltammetric determination of the drug in pharmaceuticals and human serum. *Analytica Chimica Acta*, **462** (1), 49-57.

Vidya, C., Shilpa, H., Chandraprabha, M., Lourdu, A., Indu, V., Aayushi, J., and Kokil, B. (2013) Green synthesis of ZnO nanoparticles by *Calotropis Gigantea International Journal of Current Engineering and Technology* **1**: 2277 – 4106.

Vincent, B. (1995). Electrically conducting polymer colloids and composites.*Polymers for Advanced Technologies*, **6:** 356-361.

Wang, C. and W. Zhang (1997) Nanoscale metal particles for dechlorination of PCE and PCBs. *Environmental Science and Technology*. **31** (7), 2154-2156.

Watt I.M., (1985) The Principles and Practice of Electron Microscopy. Cambridge Univ. Press. Cambridge, England.

Wang, J., Munir, A., and Zhou, H. S. (2009). Au NPs-aptamer conjugates as a powerful competitive reagent for ultrasensitive detection of small molecules by surface plasmon resonance spectroscopy. *Talanta*, **79** (1), 72-76.

Wang, T., Jin, X., Chen, Z., Megharaj, M., and Naidu, R. (2014). Green synthesis of Fe nanoparticles using eucalyptus leaf extracts for treatment of eutrophic wastewater. *Science of the Total Environment*, **466**, 210-213.

Williams, D. B., and Carter, C. B. (1996). *The transmission electron microscope* (pp. 3-17), Springer USA.

Yau, Y. C., Peacor, D. R., & McDowell, S. D. (1987). Smectite-to-illite reactions in Salton Sea shales: A transmission and analytical electron microscopy study. *Journal of Sedimentary Research*, **57** (2).

Yigit, M. V., Mazumdar, D., and Lu, Y. (2008). MRI detection of thrombin with aptamer functionalized superparamagnetic iron oxide nanoparticles. *Bioconjugate chemistry*, *19* (**2**), 412-417.

Zeck, A., Eikenberg, A., Weller, M. G., and Niessner, R. (2001). Highly sensitive immunoassay based on a monoclonal antibody specific for (4-arginine) microcystins. *Analytica Chimica Acta*, **441**: 1-13.

Zhang, J., Chen, P., Wu, X., Chen, J., Xu, L., Chen, G., & Fu, F. (2011). A signal-on lectrochemiluminescence aptamer biosensor for the detection of ultratrace thrombin based on junction-probe. *Biosensors and Bioelectronics*, **26**: 2645-2650.

Zhao, H., Wallace, G. G., and Smyth, M. (1999). Conducting electroactive polymer-based biosensors. *TrAC Trends in Analytical Chemistry*, **18 (**4), 245-251.

Zhao, J., Lin, F., Yi, Y., Huang, Y., Li, H., Zhang, Y., & Yao, S. (2012). Dual amplification strategy of highly sensitive thrombin amperometric aptasensor based on chitosan–Au nanocomposites. *Analyst*, *137* (**15**), 3488-3495.

Zhou, L., Wang, J., Li, D., and Li, Y. (2014). An electrochemical aptasensor based on gold nanoparticles dotted graphene modified glassy carbon electrode for label-free detection of bisphenol A in milk samples. Food chemistry, **162**, 34-40.